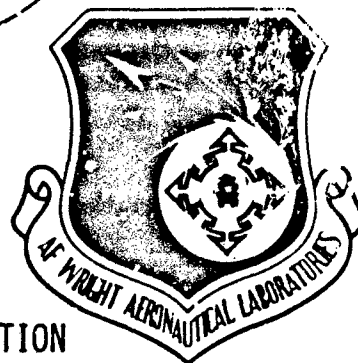


AFWAL-TR-83-4158

(12)



AD-A146 047

A STUDY OF DEFECTS IN NEUTRON TRANSMUTATION  
DOPED SILICON:GALLIUM BY HALL EFFECT ANALYSIS

Richard A. Gassman and W. C. Mitchel  
Laser & Optical Materials Branch  
Electromagnetic Materials Division

July 1984

Interim Technical Report Period: Oct 82 through Oct 83

Approved for Public Release; Distribution Unlimited

DTIC FILE COPY

Reproduced From  
Best Available Copy

MATERIALS LABORATORY  
AIR FORCE WRIGHT AERONAUTICAL LABORATORIES  
AIR FORCE SYSTEMS COMMAND  
WRIGHT-PATTERSON AIR FORCE BASE, OHIO 45433

DTIC  
ELECTE  
OCT 1 1984  
A

84 . 09 27 027

20000802240

NOTICE

When Government drawings, specifications, or other data are used for any purpose other than in connection with a definitely related Government procurement operation, the United States Government thereby incurs no responsibility nor any obligation whatsoever; and the fact that the government may have formulated, furnished, or in any way supplied the said drawings, specifications, or other data, is not to be regarded by implication or otherwise as in any manner licensing the holder or any other person or corporation, or conveying any rights or permission to manufacture use, or sell any patented invention that may in any way be related thereto.

This report has been reviewed by the Office of Public Affairs (ASD/PA) and is releasable to the National Technical Information Service (NTIS). At NTIS, it will be available to the general public, including foreign nations.

This technical report has been reviewed and is approved for publication.

*Melvin C. Ohmer*

MELVIN C. OHMER  
Work Unit Monitor  
Laser & Optical Materials Branch

*Walter L. Knecht*

for G. EDWARD KUHL - Chief  
Laser & Optical Materials Branch  
Electromagnetic Materials Division

FOR THE COMMANDER

*Merrill L. Minges*

MERRILL L. MINGES, Chief  
Electromagnetic Materials Division  
Materials Laboratory  
Air Force Wright Aeronautical Laboratories

"If your address has changed, if you wish to be removed from our mailing list, or if the addressee is no longer employed by your organization please notify AFWAL/MLPO, W-PAFB, OH 45433 to help us maintain a current mailing list".

Copies of this report should not be returned unless return is required by security considerations, contractual obligations, or notice on a specific document.

UNCLASSIFIED

SECURITY CLASSIFICATION OF THIS PAGE (When Data Entered)

| REPORT DOCUMENTATION PAGE   |                                     | READ INSTRUCTIONS<br>BEFORE COMPLETING FORM   |
|---|-------------------------------------|---|
| 1. REPORT NUMBER<br>AFWAL-TR-83-4158  | 2. GOVT ACCESSION NO.<br>AD-A146047 | 3. RECIPIENT'S CATALOG NUMBER   |
| 4. TITLE (and Subtitle)<br>A STUDY OF DEFECTS IN NEUTRON TRANSMUTATION DOPED SILICON:GALLIUM BY HALL EFFECT ANALYSIS  |                                     | 5. TYPE OF REPORT & PERIOD COVERED<br>Interim Technical Report<br>Oct 82 through Oct 83                                       |
| 7. AUTHOR(s)<br>Richard A. Gassman<br>W. C. Mitchel   |                                     | 6. PERFORMING ORG. REPORT NUMBER  |
| 9. PERFORMING ORGANIZATION NAME AND ADDRESS<br>Materials Laboratory (AFWAL/MLPO)<br>Air Force Wright Aeronautical Laboratories, AFSC<br>Wright-Patterson AFB, OH 45433  |                                     | 8. CONTRACT OR GRANT NUMBER(s)  |
| 11. CONTROLLING OFFICE NAME AND ADDRESS<br>Materials Laboratory (AFWAL/MLPO)<br>Air Force Wright-Aeronautical Laboratories, AFSC<br>Wright-Patterson AFB, OH 45433  |                                     | 10. PROGRAM ELEMENT, PROJECT, TASK AREA & WORK UNIT NUMBERS<br>PE 61102F, Project 2306,<br>Task 2306Q1, Work Unit<br>2306Q106 |
| 14. MONITORING AGENCY NAME & ADDRESS (If different from Controlling Office)   |                                     | 12. REPORT DATE<br>July 1984  |
|   |                                     | 13. NUMBER OF PAGES<br>57   |
|   |                                     | 15. SECURITY CLASS. (of this report)<br>Unclassified  |
|   |                                     | 15a. DECLASSIFICATION/DOWNGRADING SCHEDULE  |
| 16. DISTRIBUTION STATEMENT (of this Report)<br>Approved for public release; distribution unlimited.   |                                     |   |
| 17. DISTRIBUTION STATEMENT (of the abstract entered in Block 20, if different from Report)  |                                     |   |
| 18. SUPPLEMENTARY NOTES   |                                     |   |
| 19. KEY WORDS (Continue on reverse side if necessary and identify by block number)<br>Silicon, neutron transmutation doping, p-type, Hall effect, gallium   |                                     |   |
| 20. ABSTRACT (Continue on reverse side if necessary and identify by block number)<br>> Temperature-dependent Hall effect analysis has been used to study neutron transmutation doped, p-type silicon conventionally doped with gallium. Moderate temperature anneals of the irradiated material produced three shallow acceptor levels. The first, at 0.57 ev., was detected after prolonged anneals at 525 C and has been identified as the Ga-X level, a substitutional gallium-substitutional carbon complex. The other two levels appeared after anneals at 600 C. These acceptors, at 0.027 and 0.040 ev., are the levels labeled A <sub>1</sub> |                                     |   |

DD FORM 1473 EDITION OF 1 NOV 65 IS OBSOLETE

1 JAN 73

UNCLASSIFIED

SECURITY CLASSIFICATION OF THIS PAGE (When Data Entered)

UNCLASSIFIED

SECURITY CLASSIFICATION OF THIS PAGE(When Data Entered)

20. Abstract (Continued)

and  $A_2$  respectively by M. Young and co-workers. Investigation of the temporal dependence of the annealing reveal these acceptor levels to be complex in nature. Substitutional gallium-devacancy complexes have been proposed as being responsible for these levels.

UNCLASSIFIED

SECURITY CLASSIFICATION OF THIS PAGE(When Data Entered)

## TABLE OF CONTENTS

| SECTION  | PAGE |
|--|------|
| I INTRODUCTION                                   | 1    |
| II BACKGROUND                                    | 5    |
| 1. Photon Detection Process                      | 5    |
| 2. Neutron Transmutation Doping Processes        | 7    |
| III HALL EFFECT                                  | 12   |
| 1. Hall Effect and Resistivity                   | 12   |
| 2. Charge Balance Equation                       | 17   |
| 3. Fitting Procedure                             | 20   |
| IV EXPERIMENTAL DETAILS                          | 26   |
| 1. Material and Irradiation                      | 26   |
| 2. Annealing Procedures                          | 26   |
| 3. Ohmic Contacts                                | 28   |
| 4. Hall Coefficient and Resistivity Measurements | 29   |
| V RESULTS  | 34   |
| VI DISCUSSION                                    | 42   |
| VII CONCLUSIONS                                  | 48   |
| REFERENCES                                       | 50   |



|     |  |
|-----|--|
| A-1 |  |
|-----|--|

## LIST OF ILLUSTRATIONS

| FIGURE |   | PAGE |
|--------|---|------|
| 1      | Hall Effect   | 13   |
| 2      | Various Voltage and Current Probe Positions for a van der Pauw Sample             | 15   |
| 3      | Log $\rho$ vs. $1000/T$ for a Si:Ga Sample Showing all Three Regions              | 22   |
| 4      | Data and Fit for an NTD Si:Ga Sample, One Acceptor Level Fit                      | 24   |
| 5      | Data and Fit for Sample in Fig. 4, Two Acceptor Level Fit                         | 25   |
| 6      | Guarding System for Resistivity and Hall Coefficient Measurements                 | 30   |
| 7      | Resistivity and Hall Coefficient Measurement System                               | 31   |
| 8      | Sample Holder   | 32   |
| 9      | Dewar Support System  | 33   |
| 10     | Concentration of Centers vs. Anneal Time, 450 C                                   | 35   |
| 11     | Concentration of Centers vs. Anneal Time, 525 C                                   | 36   |
| 12     | Concentration of Centers vs. Anneal Time, 600 C                                   | 38   |
| 13     | Effect of Temperature and Time on the Annealing for Donors in NTD, p-type Silicon | 39   |
| 14     | One-Hour Anneal Results for NTD, p-type Silicon                                   | 41   |
| 15     | Structure of $V_2$ , Ga-V and Ga- $V_2$   | 46   |

LIST OF TABLES

| TABLE |   | PAGE |
|-------|---|------|
| 1     | Fitting Results for NTD Silicon Sample NT2-11-1 | 23   |
| 2     | Hall Effect Analysis of As-grown Si:Ga Material | 27   |
| 3     | Irradiation of Si:Ga                            | 27   |
| 4     | Reactor Properties                              | 27   |
| 5     | 450 C Anneal Fitting Results                    | 35   |
| 6     | 525 C Anneal Fitting Results                    | 36   |
| 7     | 600 C Anneal Fitting Results                    | 38   |
| 8     | Isochronal Anneal Results, One-Hour Anneals     | 41   |

SECTION I  
INTRODUCTION

In recent years, extrinsic silicon has received interest as a possible infrared detector material. The wavelength response of doped silicon can be tuned to a specific band by selecting a dopant that will provide an energy level near the desired infrared (IR) band. Gallium doped silicon is a p-type semiconductor which is sensitive to the 8-12 micrometer band, where tactical, forward-looking infrared (FLIR) systems are designed to operate. These systems require a large array of detectors to produce a usable image which can be displayed on a television-like screen.

The existence of a highly developed technology for the fabrication of integrated electronics on silicon is the main reason for seeking a suitable detector material in silicon, because the arrays and concomitant processing electronics can be built on a single chip. The quality of the image from such an array is controlled by the uniformity of response and the size of each detector, or pixel. Any change in brightness across the image should be due to a corresponding change in the temperature of the object or objects being viewed, that is, a uniform background illumination should produce a uniform image. Undesirable spots can be produced by nonuniformities in the detector material and nonuniformities in the primary dopant or other electrically active impurities.

Any uniformity problem in the starting material is intensified by the large number of pixels needed to produce an image with the required resolution. Each array has as many as a thousand pixels each and up to thirty of these arrays are fabricated on each wafer. Clearly, uniformity must be built into the material to avoid the excessive cost of individually selecting or adjusting individual detectors after processing.

Besides uniformity, purity is also a serious material requirement. Residual impurities in detector grade silicon can seriously degrade the performance of the individual detectors. In photoconductive detectors, a flux of photons in the IR band of interest produces a reduction in the resistance of the detector which is monitored by the processing electronics. To achieve high gain, the resistivity of the detector in the dark must be extremely high. Because of thermal excitation of electrical carriers in semiconductors, IR detectors must be cooled to a temperature where thermal carriers are negligible.

For silicon with a single dopant, this temperature is directly related to the activation energy of the dopant: the lower the activation energy, the lower the temperature must be before "freeze-out" is achieved. For gallium-doped silicon, with an activation energy of about 0.073 ev., freeze-out occurs at around 25 K. For indium-doped silicon, which has been used for the 4-5 micrometer IR band, freeze-out occurs at around 65 K because the activation energy of indium in silicon is 0.156 ev.

Purity becomes a problem when there are impurities in the material with an activation energy lower than of the primary dopant. The ubiquitous impurity boron has the lowest activation energy at 0.045 ev. of any elemental acceptor in silicon. If there is an excess of boron in p-type silicon, it will determine the freeze-out temperature rather than the primary dopant, such as gallium or indium. If a detector is operated at a temperature above the freeze-out temperature, there will be an unacceptably high dark current that will degrade the signal-to-noise ratio. Excessive boron in Si:Ga detectors can reduce the operating temperature to around 15 K. The additional cooling requirements can make the detector impractical for airborne or satellite applications.

The purity requirements for detector-grade silicon can be achieved by the application of float-zone growth technique in place of the more standard crucible Czochralski technique. The float-zone process is a contactless growth technique wherein a molten zone is passed through a

vertically suspended bar of polycrystalline material. The zone is kept small enough so that surface tension maintains the continuity of the bar. Several passes of the zone through the bar are used to zone-refine (Reference 1), the material before a seed crystal is used to initiate single crystal growth for the final pass. Unfortunately, the segregation coefficient for boron in silicon is near unity; consequently, it will not zone-refine out. Therefore, the polycrystalline starting material must be refined by other means to remove boron. State-of-the-art polycrystalline silicon now has boron concentrations below  $10^{12} \text{ cm}^{-3}$  and this is the limiting value in detector grade material. By any standard of purity this is very low, but if the residual donor impurities, such as phosphorus and arsenic, are present in lower concentrations, as is often the case owing to the preliminary zone-refining, then the boron can still lower the operating temperature.

During crystal growth, the crystal and polycrystal boule are counter-rotated to maintain diameter control. This rotation seems to be the major limitation of the growth process because it interacts with the thermally induced convection currents in the melt to produce fluctuations in dopant and impurity concentrations, which can produce corresponding inhomogeneities in detector response. Because of its segregation coefficient, boron is hardly affected by these convection currents, but the residual donors are strongly affected; thus, there can be regions in the material where the donor concentration exceeds the boron concentration, and other regions where the reverse is the case. One way to eliminate this effect is to intentionally add donors, such as phosphorus, along with the gallium to ensure that the boron is overcompensated throughout the boule, but there will still be variations in the donor concentration and these can produce variations in the carrier lifetime of the detectors. This results because the concentration of donors determines the concentration of ionized acceptors in p-type material at low temperatures. These ionized acceptors are the primary lifetime-limiting trap sites.

Another method of avoiding the variations in boron concentration, which is the basis of this report, is to use neutron transmutation doping (NTD)<sup>2</sup> to add phosphorus to a boule after growth. In this process, the isotope  $^{30}\text{Si}$  is transmuted into  $^{31}\text{P}$  by the absorption of a thermal neutron from the neutron flux of a nuclear reactor. Because the neutron capture cross section of  $^{30}\text{Si}$  is relatively low, the doping is very uniform and can be controlled quite accurately once the flux of the reactor is characterized. This technique (References 3, 4) has been widely used for doping silicon for use in discrete high power devices where uniformity is an important requirement. The technique is now being used to counter dope detector-grade material as well (Reference 5). The standard procedure for detector silicon is to add phosphorus to about five times the boron concentration. This amount is high enough to ensure that the temperature dependence of the material is determined by the primary dopant but low enough so as not to adversely affect the lifetime. This is by far the most uniform doping technique available today, but NTD does have some disadvantages. These derive from the fact that the neutron irradiation produces lattice damage that must be annealed out before the material can be used for device fabrication.

Studies at Hughes Research Laboratories (HRL) by Mary Young and co-workers (References 6, 7, 8) revealed two extremely shallow acceptor states at 0.027 and 0.040 eV. in NTD Si after annealing in 600 C for 1 hour. We have verified the existence of these states in HRL-grown Si:Ga as well as that grown at other laboratories. In addition, we have discovered the Ga-X level in NTD material at lower anneal temperatures. This research is reported herein.

The report is organized as follows. Section II presents background material, including a general discussion of the NTD process and irradiation damage in silicon in general. Section III discusses of the Hall effect as well as the fitting procedure used for the data. Experimental details are given in Section IV. The results are presented in Section V and discussed in Section VI, and the conclusions are given in Section VII.

## SECTION II

## BACKGROUND

## 1. PHOTON DETECTION PROCESS

A semiconductor is a material in which the valence band is full of electrons, the conduction band is empty and the forbidden gap between them is relatively narrow. For the material to become electrically conductive, electrons must be transferred into the conduction band or out of the valence band. If the material is sufficiently pure, the only way either of these events can occur is for the crystal lattice to be given enough energy to excite an electron from the valence band to the conduction band. This then leaves an electron in the upper conduction band and a hole, or absence of an electron, in the valence band, both of which can conduct electricity. When a material conducts because of an equal number of electrons and holes, it is called an intrinsic material. The energy to excite the electrons across the gap is most often supplied in one of two ways. If the thermal energy in the lattice is high enough, electrons can be excited across the gap by absorbing a phonon of sufficient energy. Another source of energy is an external electromagnetic field. If light of a short enough wavelength is incident on the material, electrons can absorb a photon and jump the gap. For most semiconductors, with gap energies around an electron volt or greater, the corresponding wavelength of light required is in the red or near infrared region of the spectrum.

Another type of conduction, extrinsic, occurs when only one type of carrier dominates the conduction process in a semiconductor. This can only occur in an impure or damaged semiconductor. Many impurity atoms, those with different valence states from silicon in particular, produce states in the forbidden gap. Atoms with more valence electrons than silicon's four produce donor states which can add an electron to the conduction band if energy is supplied. Acceptor states are produced by atoms with fewer than four and these can remove an electron from the valence band producing a hole. These states in the forbidden gap

require less energy to put a carrier in one of the bands than is required to excite an electron across the whole gap and so the wavelength response of extrinsic silicon can be tuned to a given band in the infrared. Of course, for conduction to be dominated by the photo-excited carriers, as is required in IR detectors, the thermal energy must be low enough so that no carriers are excited by this means. This is accomplished by cooling the sample. The most common dopants for extrinsic silicon detectors are indium, with an acceptor level at 0.156 ev. for use in the 4-5 micrometer band, and gallium with an acceptor level at 0.073 ev., for use in the 8-12 micrometer band.

To a first approximation, the activation energy, or the energy required to free the electron or hole to its respective band, can be calculated by assuming that the impurity atom behaves like a simple hydrogen atom. In this hydrogenic model the ground state energy is given by (Reference 9):

$$E = \frac{m^*}{m} \frac{1}{\epsilon_0} 13.5 \text{ ev.} \quad (1)$$

where  $\epsilon/\epsilon_0$  is the dielectric constant, 11.9 for silicon, and  $m^*/m$  is the ratio of the effective mass of a free carrier in the semiconductor to the rest mass of the electron. The hydrogenic ground states for donors and acceptors in silicon are 0.0191 and 0.0384 ev., respectively. These values can be considered as the minimum values for simple impurities or defects in silicon.

When an extrinsic photoconductive infrared detector is illuminated with radiation, the conductivity increases due to the increase in photo-excited carriers, but the magnitude of the conductivity change also depends on other factors as well. This change is dependent on the thickness,  $t$ , of the sample, the photon flux,  $\phi$ , incident on the detector, the quantum efficiency,  $\eta$ , of the detector, the mobility,  $\mu$ , of the carriers and their lifetime,  $\tau$ . Of these, the quantum efficiency,

mobility and lifetime are material dependent. The change in hole concentration in a p-type detector due to an incident flux is:

$$\Delta p = \frac{\tau \phi \eta}{t} \quad (2)$$

From this, and the general expression for conductivity,  $\sigma = pe\mu$ , we get the expression for the change in conductivity, in steady state:

$$\Delta \sigma = \frac{\tau \phi \eta e \mu}{t} \quad (3)$$

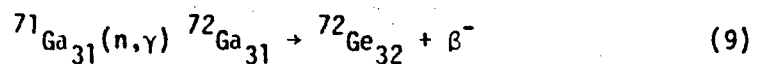
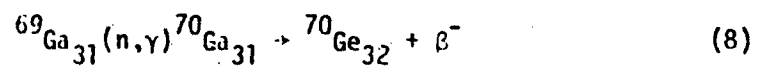
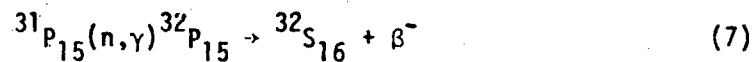
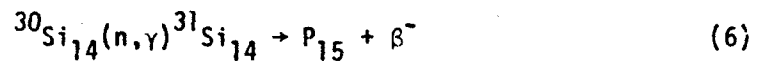
The quantum efficiency gives the number of carriers produced per incident photon and is related to the absorption cross section of the primary dopant in extrinsic material. It can change on a local scale if there is a variation in the primary dopant concentration. This is the principle cause of dark or bright spots in detector arrays. The mobility is determined by the scattering mechanisms present in the material. Phonon scattering can usually be neglected because of the low temperatures of operation. Ionized impurity scattering is the dominate mechanism determining the mobility in extrinsic detectors. The lifetime is the amount of time a carrier stays in the band before it is trapped by an ionized impurity and decays back to its ground state on the dopant atom. The ionized traps can be the primary dopant atoms, residual impurity atoms, or charged defects and are, for photon fluxes of interest, equal to the total number of donors in p-type material. Therefore, compensation of residual impurities and its uniformity can make large differences in lifetime and the uniformity of that process. It is this effect that is the primary driving force of this research effort.

## 2. NTD PROCESSES

### a. Nuclear Reactions

In neutron transmutation doping, or NTD, an isotope of one element is transmuted into another element by the absorption of a thermal neutron which is usually supplied by the neutron flux of a reactor.

For this process to be technologically feasible, the first isotope must have a reasonable concentration in the host material and the new element must be a desired dopant in the host. In addition, no other unwanted elements may be produced in measurable quantities. All these restrictions are met in silicon. The isotope  $^{30}\text{Si}_{14}$  has a relative abundance of 3% in natural silicon and transmutes into  $^{31}\text{P}_{15}$ , which is a standard donor element in silicon, by beta emission with a half-life of 2.62 hrs. The other isotopes of Si transmute into heavier Si isotopes and so do not affect the doping. The principle reactions for Si:Ga are given below:



Processes 7, 8 and 9 are all second order and can be neglected.

The relatively small capture cross section of silicon for thermal neutrons ( $1.676 \times 10^{-4} \text{ cm}^2$ ) ensures that the doping will be uniform because the flux is not appreciably degraded as it passes through even a large diameter boule. In fact, NTD of silicon is by far the most uniform method available, as evidence by its widespread use in the high-power thyristor industry, where uniformity is the most important material parameter. The uniformity of phosphorus doping is also valuable in detector materials as well. Here, NTD is often used to overcompensate residual boron. The boron is reasonably uniformly distributed but the

residual donors are not. This leads to serious local variations in trap concentrations. If NTD is used to overcompensate the boron by a factor of 5 or so, all residual inhomogeneities are swamped out by the NTD phosphorus.

b. Radiation Damage

There are several disadvantages to the NTD process; the principal one being the lattice damage that is left after irradiation. Most reactor fluxes have a certain percentage of non-thermalized, fast neutrons with energies in excess of 0.1 Mev. This part of the flux does not contribute to the transmutation process but rather causes considerable damage due to primary collisions with silicon atoms and secondary collisions of these atoms with others nearby. Fast neutrons create large, complex, disordered regions that can be up to 10 micrometers in length (Reference 10). In addition to their damage, there is also lattice disruption caused by the recoil of atoms after beta decay and gamma emission. All this damage must be annealed out before devices can be made from the material. The usual recipe is to anneal the irradiated material at 750-850 C for 1 to 2 hours. This appears to remove the majority of the damage and activate the NTD phosphorus which was originally in a nonactive interstitial position; owing to recoil of the atom at the time of transmutations.

Many of the complexes that form during irradiation or low-temperature anneals are quite complex and quite often are electrically active, that is, they are donors or acceptors, or both. In NTD material, it is these damage levels that dominate the electrical properties of the material until they are removed by annealing. A study of the time and temperature dependence of the annealing of these levels can often give valuable information on their identification. The Hughes levels (References 6, 7 and 8) are such damage levels but appear unique in that they are extremely shallow, or close to the band. This is not usually the case with most complexes, which are most often found nearer to the middle of the gap. To understand how these shallow levels are formed and

what they are, we must understand the mechanisms for the production and disruption of complexes in silicon by irradiation and subsequent annealing.

In metals, vacancies play a fundamental role in explaining damage recovery and diffusion mechanisms because of the large number of vacancies that are in thermal equilibrium at high temperatures. By annealing, the energies of formation and migration of the vacancies can be determined. In metals, these energies are about 1.0 ev. However, in semiconductors like silicon, the energy of formation is approximately 2.35 ev. and the energy of migration is approximately 0.3 ev. The energy of formation for a single vacancy in silicon is this large because the silicon forms a diamond lattice with covalent bonds which are very strong. Four of these bonds must be broken to form a vacancy. This also explains why vacancies migrate so much faster. The large strain on the lattice due to the vacancy forces it to move quickly out to a sink and disappear. Vacancies in silicon have moved down to 4.2 K (Reference 11). For these reasons, it is very difficult to have a single vacancy in thermal equilibrium at room temperature. If vacancies are present they are generally complexed with impurities or other vacancies. They are not generated thermally until almost at the melting point of silicon. This all makes diffusion by a vacancy mechanism very unlikely.

A more likely mechanism for solute diffusion in silicon is the interstitial mechanism. The diamond lattice in silicon is relatively open. This gives enough room for atoms to move through the relatively large interstitial corridors of the diamond lattice. The diffusion of acceptors in silicon has been attributed to a replacement mechanism in which a substitutional solute atom jumps to an interstitial site, a neighboring solvent atom jumps into the resulting vacancy, and the interstitial solute atom moves into the new vacancy (Reference 11). Interstitial silicon atoms in silicon have a migration energy of approximately 0.2 ev., which implies rapid mobility interstitially.

Although vacancies are not in thermal equilibrium in silicon at temperatures below the melting point, they can be generated by a number of different mechanisms and, as previously mentioned, are extremely mobile. NTD creates a great deal of damage in silicon, including vacancies. These vacancies interact with impurity atoms and each other to create impurity-vacancy complexes and vacancy clusters. If the vacancy complexes start to dissociate, even at a low temperature, the vacancies will tend to migrate to sinks unless trapped by other centers. Silicon interstitials are also not in equilibrium and can get trapped by impurities and dopants in an interstitial site next to the solute atom. With enough thermal energy, a silicon atom will eject the solute atom to an interstitial position and replace it on the substitutional site. This mechanism has been called the Watkins replacement mechanism (Reference 11). The interstitial solute atom is then free to interact with interstitial solvent atoms and impurities as well as substitutional atoms to form various complexes. Many such complexes are relatively stable and are seen in anneals beyond 400 C. Other complexes can be formed as the solute atoms return to substitutional positions in the lattice. The Ga X-level is believed to be such a complex. At present, this level is thought to be a substitutional gallium-substitutional carbon pair. The carbon atom, normally not electrically active, distorts the lattice around the gallium and in doing so lowers the energy of the gallium ground state (Reference 12). This type of level has been seen to be produced by both electron and neutron irradiation (References 13, 14).

## SECTION III

## HALL EFFECT

## 1. HALL EFFECT AND RESISTIVITY MEASUREMENTS

The Hall effect (References 15,16) is often used in semiconductor research to determine the concentrations of electrically active centers. In this effect, a voltage is produced perpendicular to the direction of both an applied current and magnetic field which are themselves mutually perpendicular, as shown in Figure 1. The magnetic field induces a Lorentz force on the moving charge carriers perpendicular to the current. In steady-state, there can be no net force on the carriers, so an excess concentration of charges is built up on the edge of the sample until an electrostatic field is generated which balances the Lorentz force. This field is called the Hall field. For a constant magnetic field, the current and Hall voltage are related by an Ohm's Law type expression:

$$V_H = R_H \frac{IH}{t} \quad (10)$$

where  $V_H$  is the Hall voltage,  $I$  and  $H$  are the applied current and magnetic field and  $t$  is the thickness.  $R_H$  is the Hall coefficient. In the high magnetic field limit, where  $R_H$  can be shown to be independent of the magnetic field, it is given by:

$$R_H = -\frac{1}{ne} \text{ or } \frac{1}{pe} \quad (11)$$

depending on whether the conduction is by electrons ( $n$ ) or holes ( $p$ ).  $n$  and  $p$  are the respective carrier concentrations. For arbitrary magnetic fields,  $R_H$  can be expressed as:

$$R_H = -\frac{r_e}{ne} \text{ or } \frac{r_h}{pe} \quad (12)$$

where  $r_e$  and  $r_h$  are the scattering factors for electrons and holes, respectively. The parameter  $r$  is, in general, a function of the scattering mechanisms, the band structure, temperature, and the

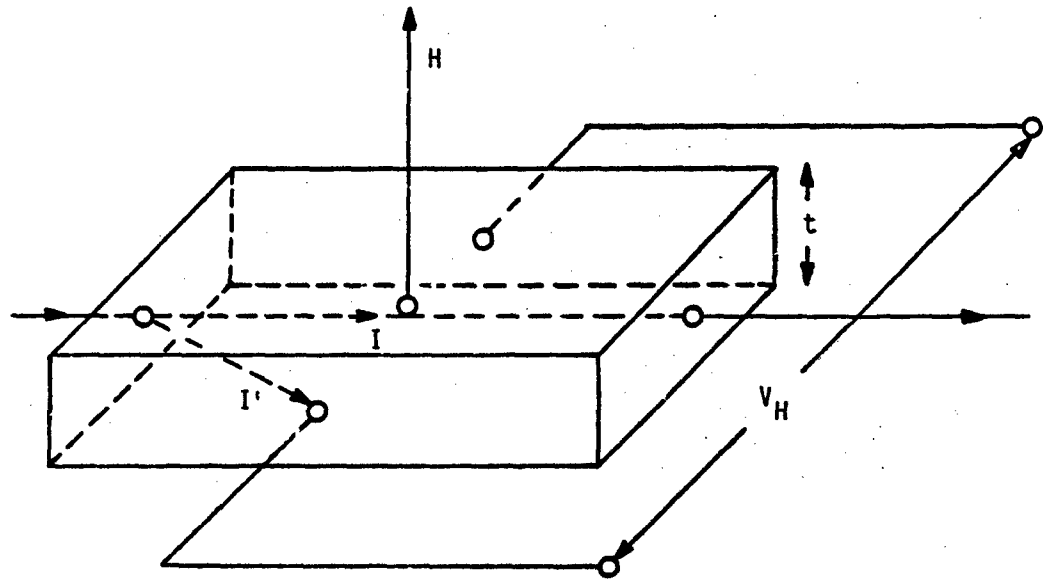


Figure 1. The Hall Effect,  $i$  is the applied current,  $i'$  is the deflected charge path,  $H$  is the applied magnetic field and  $V_H$  is the induced Hall Voltage,  $t$  is the sample thickness

magnetic field strength, but is usually on the close order of unity and can often be neglected in analysis if precision of better than 50 percent is not needed.

If  $R_H$  is determined experimentally by use of Equation 3.1 and  $r$  is known, then Equation 3.3 can be used to determine the carrier type and concentration. In extrinsic semiconductors, the carrier concentration can be related to the probability of occupation of the various levels contributing to the carrier concentration. This probability is given by a sum over a Fermi-Dirac type expression for each level. Therefore, if the Hall coefficient is measured as a function of temperature, detailed information can be obtained on the energy levels that contribute to the conduction process. In particular, both the concentration and activation energy of several levels can be determined by fitting the theoretical expression for the carrier concentration to the  $R_H$  data. The actual fitting procedure is discussed in the next section.

The method used in this experiment to measure the Hall coefficient and resistivity is that suggested by L. J. van der Pauw (Reference 17). In this method, four contacts are placed on the periphery of an arbitrarily shaped sample, as shown in Figure 2(a). A pair of voltage probes and a pair of current leads are attached to the four contacts, as shown in b, c, and d of Figure 2. If the lead configuration shown in b is called position #1 and that in c is called position #2, we can define resistances  $R_1$  and  $R_2$  as  $V_{AB}/I_{CD}$  and  $V_{BC}/I_{AD}$  respectively where  $V_{ij}$  is voltage measured across points  $i$  and  $j$  and  $I_{kl}$  is the current applied between points  $k$  and  $l$ . It was shown by van der Pauw that the resistivity of the sample is given by:

$$\rho = \frac{\pi d}{2 \ln 2} (R_1 + R_2) f(R_1/R_2) \quad (13)$$

where  $f(x)$  is given by the expansion:

$$f(x) = 1 - \left(\frac{x-1}{x+1}\right)^2 \frac{\ln 2}{2} - \left(\frac{x-1}{x+1}\right)^4 \left( \left(\frac{\ln 2}{12}\right)^2 - \left(\frac{\ln 2}{12}\right)^3 \right) + \dots \quad (14)$$

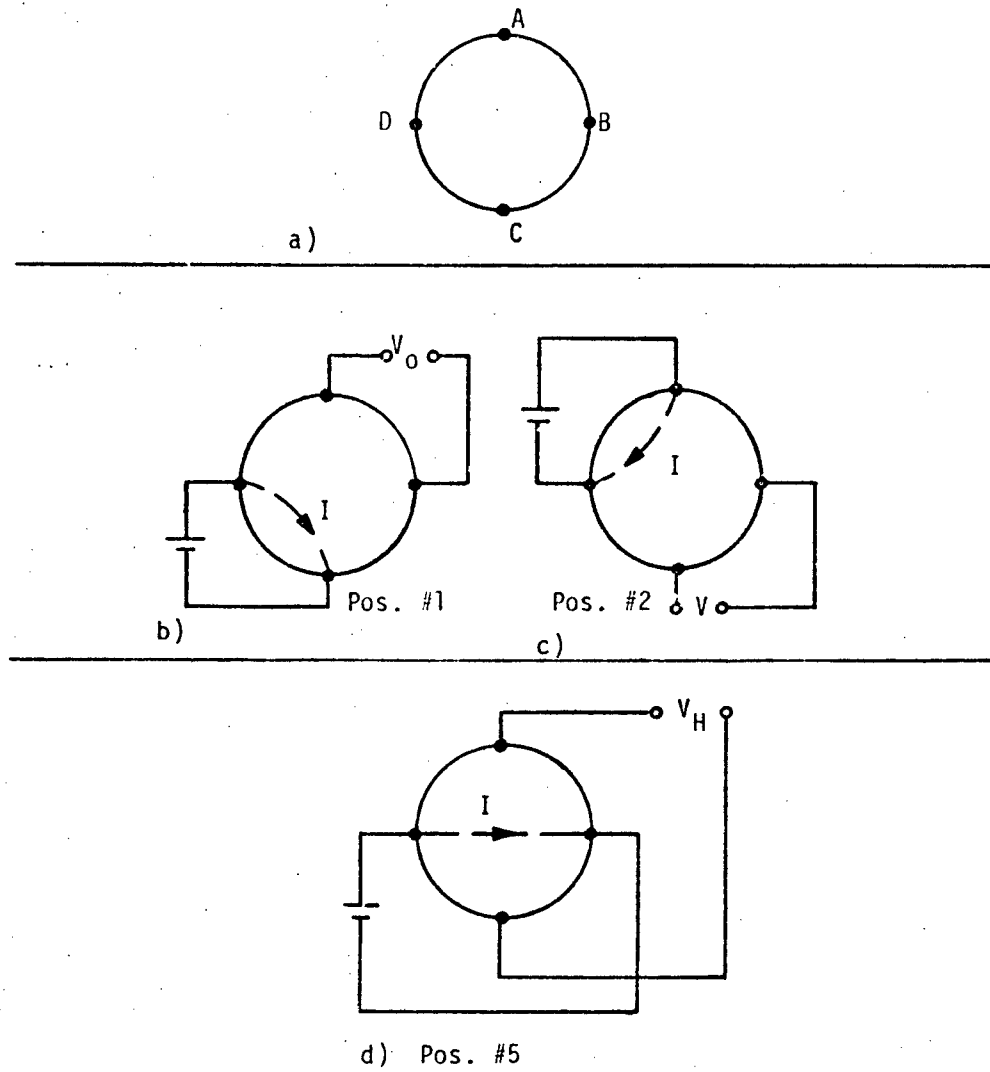


Figure 2. Various voltage and current probe positions for a van der Pauw sample. b and c are used for resistivity and d is used for Hall coefficient measurements

The beauty of the van der Pauw technique is that all the geometrical effects are taken into account with a single universal function of two resistance measurements. The only sample dimension that has to be measured is the thickness, so many of the problems that plague conventional resistance measurements are eliminated. There are some limitations, however. The four contacts must be on the periphery of the sample and be small compared to the dimensions of the sample. In addition, the sample itself must be of a uniform thickness and non-reentrant, i.e., there can not be any holes in the sample.

Real contacts on a sample are rarely on the actual periphery and can be of significant size. The magnitude of the error such contacts produce can be estimated by the expression (Reference 17):

$$\frac{\Delta\rho}{\rho} = \frac{d^2}{4D^2 \ln 2} \quad (15)$$

This expression assumes a circular sample and circular contacts where  $\rho$  is the resistivity,  $d$  is the diameter of the contact, and  $D$  is the diameter of the sample. For contacts of 1 mm in diameter on a 6.25 mm-diameter sample, the error is only about 2%. The error can be reduced further if slits are cut in the sample, making a cloverleaf shape. The slits increase the path length of the current from contact to contact which increases the effective diameter of the sample. Using the same expression, but assuming that the diameter of the sample is approximately equal to the length of the diagonal on 1/4-inch-square sample, the error is only 0.9%. All samples used in this experiment were square cloverleaves with 1/4-inch sides. The contacts were made on the corners and kept as small as possible.

The Hall coefficient,  $R_H$ , can be measured with a van der Pauw sample if the contacts are symmetrically located on a two-fold symmetric sample with current and voltage leads in the configuration of Figure 2(d).  $R_H$  is then given by:

$$R_H = \frac{V_H t}{I_H} \quad (16)$$

$R_H$  is determined by averaging four Hall measurements. These measurements are taken in all four possible polarity combinations of magnetic field and sample current. Averaging over current directions eliminates any thermoelectric voltages due to dissimilar lead materials. Averaging over the magnetic field direction eliminates any magneto-resistance component that might be present due to non-symmetric voltage contacts. Here, the two  $R_H$ 's are subtracted because  $R_R$  is proportional to  $H$  while the magnetoresistance is dependent on only even components of  $H$ . The thermoelectric voltages are eliminated by adding resistances because they are independent of the current. Resistivity values are also averaged over the current direction as well.

As stated previously, before the carrier concentration can be precisely determined from Hall effect data, the scattering factor,  $r$ , must be known. This factor arises in the calculation because the energy surfaces of real semiconductors are not spherical and parabolic as simple theory often assumes. Unfortunately, to date the experimental and theoretical difficulties involved in determining the scattering factor have not been overcome and a completely satisfactory  $r$  is not available. Many researchers therefore assume a value of unity for  $r$ . In this experiment, an empirical scattering factor developed in the Laser & Optical Materials Branch has been used. The form used is:

$$r(T) = 0.54 + 1.22T / [50(1 + T^2/50^2)] \quad (16)$$

This expression is purely empirical and does not represent any attempt at an accurate, theoretical calculation.

## 2. CHARGE BALANCE EQUATION

To determine the concentrations and energies of the various levels in a sample from the carrier concentration data, an expression relating  $n$  or  $p$  and  $T$  to the probability of occupation of each level at any temperature must be used. Such an expression is derived below. A discussion of the procedure used in this laboratory to fit the data to that expression follows.

We start with the simplest form of the charge balance equation, an expression of the total electrical neutrality of the sample:

$$n + N_a^- = p + N_d^+ \quad (17)$$

Here  $N_a^-$  and  $N_d^+$  are the concentrations of ionized acceptors and donors, respectively. For p-type material,  $n$  can be neglected and  $N_d^+$  set equal to  $N_d$ , the total number of donors. Then:

$$p + N_d = N_a^- \quad (18)$$

If there is more than one acceptor level, one need merely sum over all of them to obtain:

$$p + N_d = \sum_i N_{a_i} \quad (19)$$

where the summation is over acceptor levels. Here a similar summation is assumed for the donors and  $N_d$  is total number of donors from all sources. We must now relate  $N_{a_i}$  to the probability of occupation of the  $i^{\text{th}}$  level. We will follow the derivation of Seeger (Reference 18).

The probability  $P_e(E)$  that a particular level at energy  $E$  will be occupied by an electron is given in the Fermi-Dirac statistics by:

$$P_e(E) = (\exp((E-E_F)/kT) + 1)^{-1} \quad (20)$$

where  $E_F$  is the Fermi energy or, equivalently, the electrochemical potential. Now, for acceptor states, a level will be occupied by a hole if it is unoccupied by an electron so the probability of an acceptor level being occupied by a hole,  $P_h(E)$ , is  $1 - P_e(E)$ , or:

$$P_h(E) = (\exp(E_F - E)/kT + 1)^{-1} \quad (21)$$

The total number of unionized acceptors of energy  $E$  is just the total number of acceptors at that energy times the probability they will be unoccupied:

$$n_a = \frac{N_a}{1 + e^{(E_F - E)/kT}} \quad (22)$$

This expression holds only for nondegenerate levels. Because of spin degeneracy, all levels will be at least two-fold degenerate. For a level with a degeneracy of  $g$ , Equation 22 takes the form:

$$n_a = \frac{N_a}{1 + \frac{1}{g} e^{(E_F - E)/kT}} \quad (23)$$

From the fact that  $N_a = n_a + N_a^-$ , we see that

$$\frac{n_a}{N_a} = g e^{(E - E_F)/kT} \quad (24)$$

Now, all we need is one more expression so that  $E_F$  can be eliminated from Equation 3.15. This elimination is accomplished by use of the general expression for the hole concentration.

$$p = N_V e^{(E_V - E_F)/kT} \quad (25)$$

where  $N_V$  is the density of states in the valence band and  $E_V$  is the top of the valence band. Now, if we divide Equation 24 by Equation 25, we obtain

$$\frac{N_a^-}{N_a} = \frac{g e^{E_a/kT}}{N_V} \quad (26)$$

where  $E_a = E - E_V$ ,  $E_a$  is the "activation energy" of the acceptor level or the energy required to remove a hole from the level to the valence band. From Equation 26, remembering that  $n_a = N_a - N_a^-$ , we immediately get:

$$N_a^- = \frac{N_a}{1 + \frac{pg}{N_V} e^{E_a/kT}} \quad (27)$$

Substituting this into Equation 19, we obtain our desired expression for the hole concentration:

$$p + N_d = \sum_i \frac{N_{a_i}}{1 + p g_i e^{E_{a_i}/kT}} \frac{N_v}{N_v} \quad (28)$$

The form of the density of states factor,  $N_v$ , is derived from the carrier concentration effective mass of Madarasz, Lang and Hemenger (Reference 19). We note that the density-of-states term in this expression is temperature dependent and is roughly proportional to  $T^{2/3}$ .

### 3. FITTING PROCEDURE

With Equation 28 and  $p$  vs.  $T$  data in hand, one can proceed to fit the data to the equation to obtain values for  $N_d$ ,  $N_{a_i}$  and  $E_{a_i}$  for, in principle at least, any number of acceptor levels. A practical limit due to density of data points and their accuracy for the number of levels is about four or five but this rarely puts any real constraints on the researcher, for it is only the rarest of samples that will have more shallow levels than this. To show the type of information that can be obtained without elaborate computer aided fitting procedures, we will first consider the charge balance equations for the case of a single, partially compensated acceptor.

For most materials, the intentional doping concentration is several orders of magnitude higher than the concentration of the compensating centers. In this situation there are three regions of interest in a plot of  $\log p$  vs.  $1000/T$ . First, at temperatures that are high enough that all the acceptors are ionized yet still low enough that there is negligible band gap excitation of electron-hole pairs,  $p$  is independent of temperature and equal to  $N_a - N_d$ . This is the saturation region. Second, as the temperature is lowered,  $p$  will become negligible

compared to  $N_a$  but still be considerably greater than  $N_d$ . For this case one may express Equation 28 in a slightly different form (for one acceptor level only):

$$\frac{p(p + N_d)}{N_a - N_d - p} = \frac{N_v}{g} e^{-E_a/kT} \quad (29)$$

Now, the above restrictions are  $N_a \gg p \gg N_d$ . Then

$$p = \sqrt{\frac{N_v N_d}{g}} e^{E_a/2kT} \quad (30)$$

We see that the slope of our plot will be one half of the activation energy times  $1000/k$ . Finally, at the lowest temperatures, the carrier concentration will be lower than either  $N_a$  or  $N_d$ ,  $N_a > N_d \gg p$ . Equation 29 reduces to

$$p = \frac{N_v (N_a - N_d)}{g} e^{-E_a/kT} \quad (31)$$

The slope is now proportional to the activation energy itself. These three regions are clearly visible in the example shown in Figure 3, which is data for a gallium-doped sample. Unfortunately, most samples do not show all three regions, so care must be taken when determining the activation energy.

When multiple levels are present, the situation is much more complex and the slopes determined from graphical analysis can be misleading. In these cases a fit to the full charge balance equation is the best procedure to follow. At this laboratory a least-squares fit similar to that of Bevington (Reference 20) is used for this purpose. Because Equation 28 is not a closed expression for  $p$ , the program performs an iterative solution at each temperature point. The program varies the parameters  $N_d$ ,  $N_{a_i}$ , and  $E_{a_i}$  against the data to minimize a reduced chi-squared defined by:

$$\chi^2 = \frac{1}{N-n} \sum_{i=1}^N \frac{(y_i - f(x_i))^2}{\sigma_i^2} \quad (32)$$

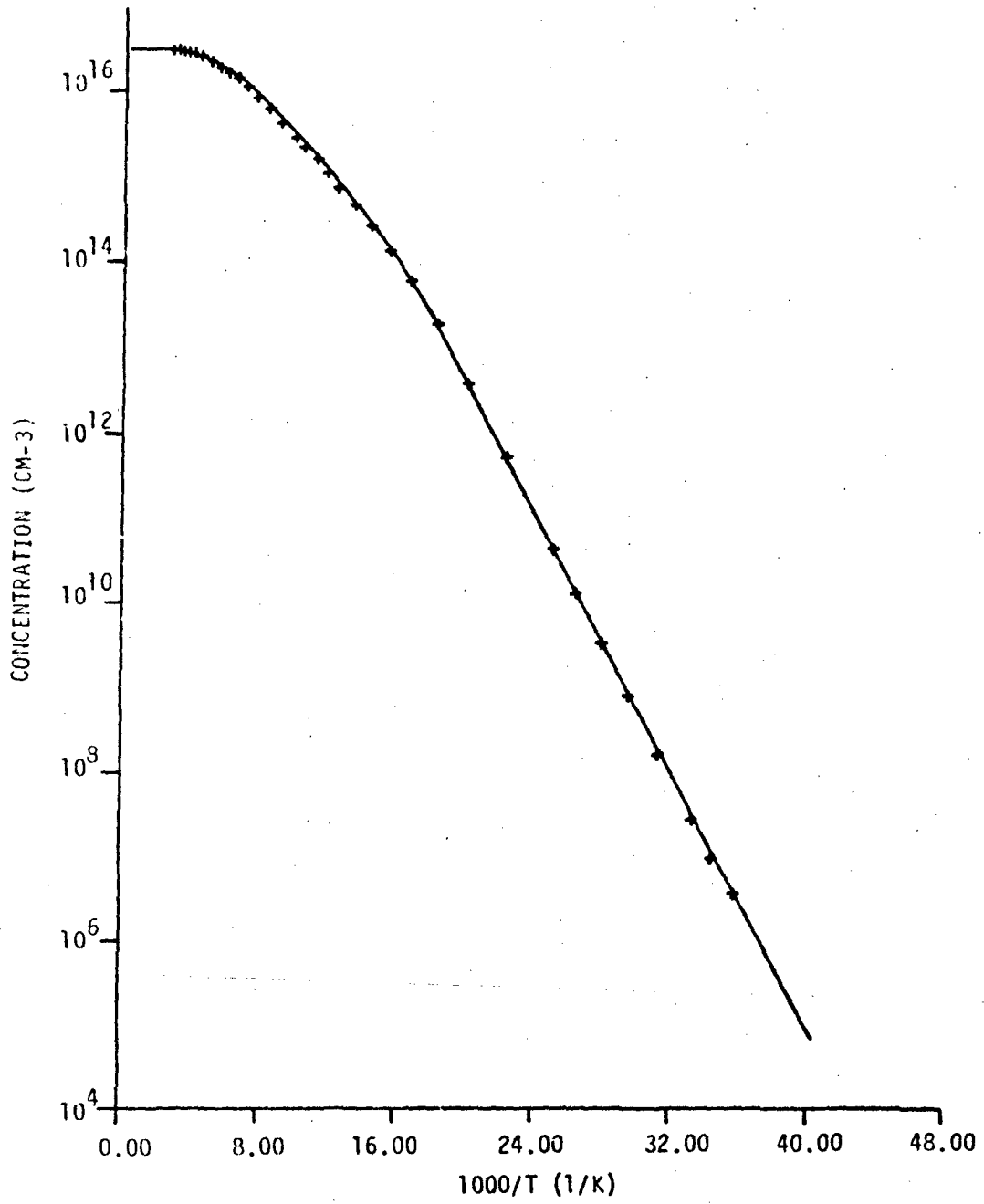


Figure 3. Log p vs 1000/T for a Si:Ga sample showing all three regions

$N_p$  is the number of data points,  $n$  is the number of adjustable parameters,  $y_i$  is the carrier concentration at data point  $i$  and  $f(x_i)$  is the corresponding value computed from the iterative solution at temperature  $T_i$ ,  $\sigma_i$  is the experimental error, assumed to be 3% of the measured carrier concentration. The program will iterate the minimization any number of times until a minimum  $\chi^2$  is found. Figures 4 and 5 show the data for one sample run with the results of two separate fitting attempts. The fit shown in Figure 4 was made assuming only one acceptor level, while that in Figure 5 assumed two acceptor levels. The two level fit is obviously the more superior. The resultant minimum  $\chi^2$  for each fit, 124 and 1.6, respectively, also indicate that the two level assumption is the correct one. The results of the two fits are given in Table 1. Analysis similar to this was performed on all Hall effect data sets used in this report.

TABLE 1  
FITTING RESULTS FOR NTD SILICON SAMPLE NT2-11-1

|        | $N_D$<br>( $\text{cm}^{-3}$ ) | $N_{A1}$<br>( $\text{cm}^{-3}$ ) | $E_{A1}$<br>(ev) | $N_{A2}$<br>(ev)      | $E_{A2}$<br>(ev) | $\chi^2$ |
|--------|-------------------------------|----------------------------------|------------------|-----------------------|------------------|----------|
| Fit 1. | $2.37 \times 10^9$            | $1.69 \times 10^{16}$            | .0537            | -                     | -                | 124      |
| Fit 2. | $3.06 \times 10^{14}$         | $3.58 \times 10^{16}$            | .0667            | $6.80 \times 10^{14}$ | .0287            | 1.6      |

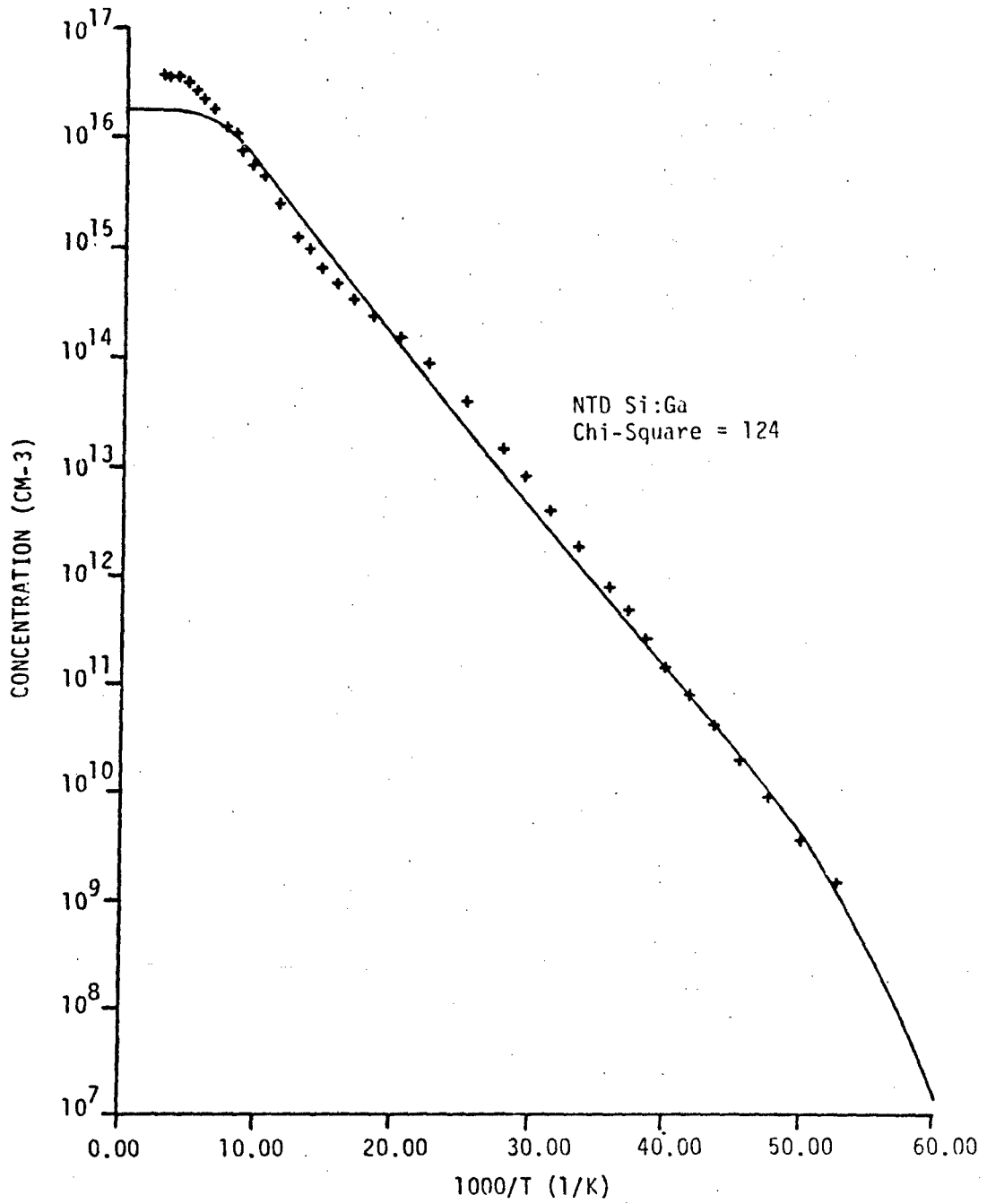


Figure 4. Data and fit for an NTD Si:Ga sample, one acceptor level fit

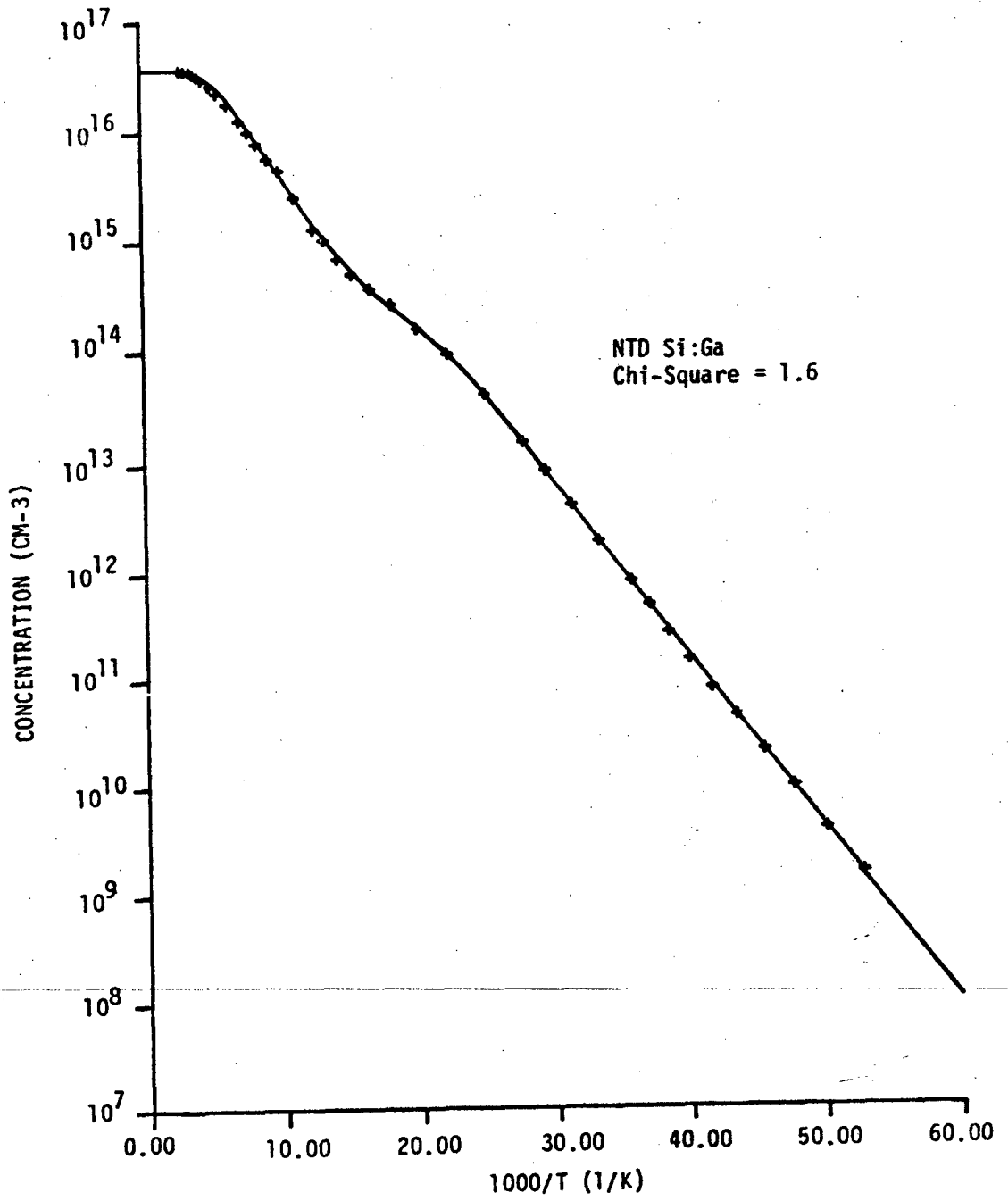


Figure 5. Data and fit for the sample in Figure 4, two acceptor level fit

## SECTION IV

### EXPERIMENTAL DETAILS

#### 1. MATERIAL AND IRRADIATIONS

The Si:Ga for this study came from three independent sources, Virginia Semiconductor (V1 and V2), Westinghouse R&D Laboratories (W1) and Hughes Research Laboratories (H1). The gallium concentrations for these boules were all in the mid  $10^{16} \text{ cm}^{-3}$  range. Boron and donor concentrations varied from boule to boule. The results of Hall effect analysis on as-grown, un-irradiated material from each boule are given in Table 2. Two different Virginia Semiconductor boules were used in this study and are labeled V1 and V2. The gallium concentration for V1 varied by as much as a factor of two between the various samples. The concentration given is the upper limit. The Hall effect measurements and analysis for H1 were performed at Hughes. This boule was supplied under the requirements of AF Contract F33615-78-C-5062. The Virginia Semiconductor material was purchased commercially. Boule W1 was donated by Dr. R. N. Thomas of Westinghouse. H1 was irradiated at Texas A&M University (TA&M) prior to delivery. These other irradiations were performed at the University of Missouri Research Reactor (MURR) where  $3 \times 10^{13}$  and  $1.2 \times 10^{14} \text{ cm}^{-3}$  phosphorus were added in different irradiations. Boule V1 was cut into samples prior to irradiation. All other material was irradiated in bulk form. The irradiations are summarized in Table 3. Table 4 gives the relevant parameters of the two reactors. The irradiation temperatures given in that table are very rough estimates and were supplied by Dr. J. M. Meese of MURR and Dr. R. Hart of TA&M. No measurements have been made of these temperatures at either reactor.

#### 2. ANNEALING PROCEDURES

After cutting and prior to all anneals, the samples were cleaned by the following procedures: Samples were rinsed successively in trichlorethylene, acetone and isopropyl alcohol. Following this, they

TABLE 2

HALL EFFECT ANALYSIS OF AS-GROWN Si:Ga MATERIAL

| Boule | $N_{Ga} (cm^{-3})$   | $N_B (cm^{-3})$      | $N_{Donors} (cm^{-3})$ |
|-------|----------------------|----------------------|------------------------|
| V1    | $6.5 \times 10^{16}$ | $5.5 \times 10^{13}$ | $1.7 \times 10^{13}$   |
| V2    | $2.0 \times 10^{15}$ | $4.4 \times 10^{12}$ | $3.5 \times 10^{12}$   |
| W1    | $3.0 \times 10^{16}$ | $2.5 \times 10^{12}$ | $6.3 \times 10^{12}$   |
| H1    | $3.0 \times 10^{16}$ | $2.0 \times 10^{13}$ | $2.0 \times 10^{13}$   |

TABLE 3

IRRADIATIONS OF Si:Ga

| Boule | Reactor | Phosphorus Added ( $cm^{-3}$ ) |
|-------|---------|--------------------------------|
| V1-a  | MURR    | $3 \times 10^{13}$             |
| V1-b  | MURR    | $1.2 \times 10^{14}$           |
| V2-a  | MURR    | $3 \times 10^{13}$             |
| W1-a  | MURR    | $3 \times 10^{13}$             |
| H1-a  | TA&M    | $5 \times 10^{13}$             |

TABLE 4

REACTOR PROPERTIES

| Reactor | Cd Ratio | Flux ( $n\ cm^{-2}$ ) | Irradiation Temperature |
|---------|----------|-----------------------|-------------------------|
| MURR    | 10-30    | $3 \times 10^{13}$    | 100 - 200°C             |
| TA&M    | 22       | $5 \times 10^{12}$    | 100°C                   |

were placed in a solution of  $\text{NH}_4\text{OH}$ ,  $\text{H}_2\text{O}_2$  and  $\text{H}_2\text{O}$  (1:1:5) at 60 C for fifteen minutes. This was followed by a fifteen minute wash in a 1:1:6 solution of  $\text{HCl}$ ,  $\text{H}_2\text{O}_2$  and  $\text{H}_2\text{O}$  at 60 C. Finally, the samples were rinsed in distilled water for at least a half hour. A similar cleaning procedure was used before each anneal for all furnace ware excepting the furnace tube.

After cleaning, the samples were placed on a high purity polycrystalline silicon furnace boat. To prevent any chance of contamination during annealing, the samples were placed between wafers of high purity silicon as well. The boat was then placed in the furnace for annealing. During annealing, argon gas was allowed to flow over the boat. A polycrystalline silicon furnace tube was used for all anneals.

### 3. OHMIC CONTACTS

Laser annealing was used to produce ohmic contacts on all samples after each anneal. A pulsed Nd:YAG laser was used to melt a few microns of the silicon surface in a 1-millimeter-diameter spot. This melting is highly localized, and there is no appreciable temperature rise of the sample. The ohmic contacts were produced by immersing the sample in a borosilicate spin-on doping solution (Reference 21) during the laser annealing procedures. The laser pulse penetrates the solution and is absorbed at the silicon surface, producing localized melting. The boron from the solution is incorporated into the silicon during recrystallization, producing a thin, degenerately doped region with low resistivity. Leads were soldered to these spots with indium solder after cleaning in soapy water and rinsing. The principal advantage of this procedure is that the bulk of the sample remains at room temperature. Other methods of producing the degenerately doped regions needed for ohmic contacts such as diffusion or ion-implantation require furnace annealing of the whole sample. Laser annealing can, of course, be used in conjunction with ion implantation but our technique gives completely satisfactory results and eliminates the implantation step.

#### 4. HALL COEFFICIENT AND RESISTIVITY MEASUREMENTS

The measurement system used in this experiment is based on the guarded approach of Hemenger (Reference 22) and Colman (Reference 23). In this system, a high-input impedance, unity gain buffer amplifier is placed between each voltage probe on the sample and the external circuitry to lower the impedance to a level below the input level of the voltmeter. In addition, the output of the buffer is used to drive the inner shield of the triaxial cable used for sample leads to the potential of the innermost lead. This reduces leakage currents and the RC time constant by eliminating stray capacitances. The arrangement used here is shown in Figure 6. The amplifiers, A, are Keithley Model 610C electrometers. The ammeter, AM, is also a 610C. The power supply, PS, that supplies the sample current, is a simple d.c. voltage source. A Hewlett Packard 3455A DVM is used to measure sample voltages. Reed relays perform all switching functions and are opened or closed electronically. The system can measure resistances up to  $10^{12}$ .

The complete Hall effect system is represented in Figure 7. The temperature is monitored by measuring the voltage drop across a reverse-biased silicon diode thermometer (Lake Shore Cryogenics Model DT500). The 10-amp current for the thermometer is supplied by a Keithley 225 constant-current source. The temperature is controlled with an Artronix 5301 which uses a combination of a carbon-glass thermometer and a platinum thermometer for sensing and drives a wire wound  $50\Omega$  heater. The sample probe is cooled in a Janis Super Veri-Temp Helium vapor dewar. The magnetic field of the Varian electromagnet is monitored with a Bell 620 Hall effect gaussmeter.

The sample holder and probe are depicted in Figure 8. The van der Pauw sample rests on a piece of high-thermal conductivity BeO and is secured with a nonmagnetic spring. The Si diode thermometer is in direct contact with the back side of the BeO. The control thermometers are positioned near the bottom heater. The two heaters are wound oppositely to reduce magnetic fields. A drawing of the dewar support system is shown in Figure 9.

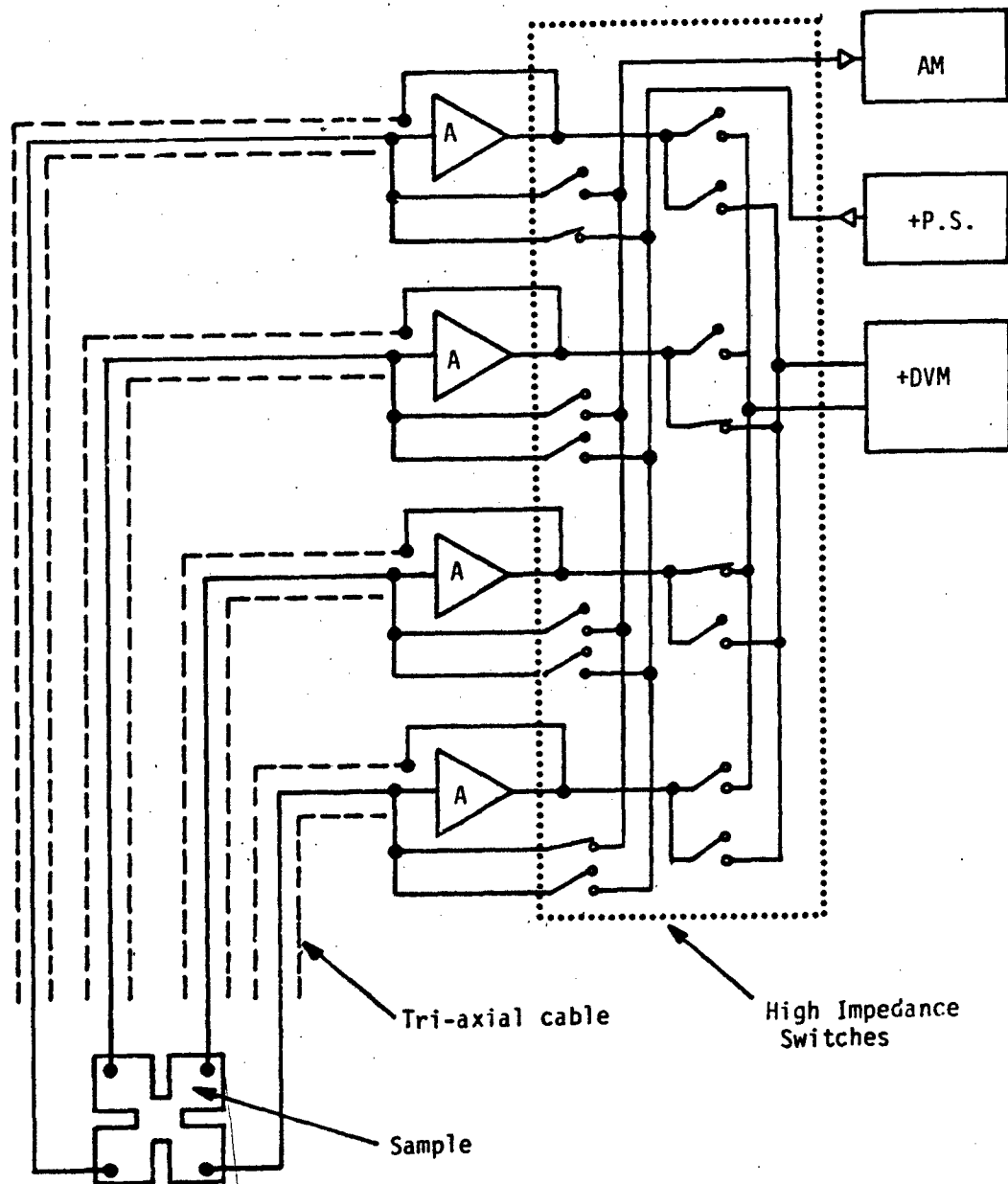


Figure 6. Guarding System for Resistivity and Hall Coefficient Measurements

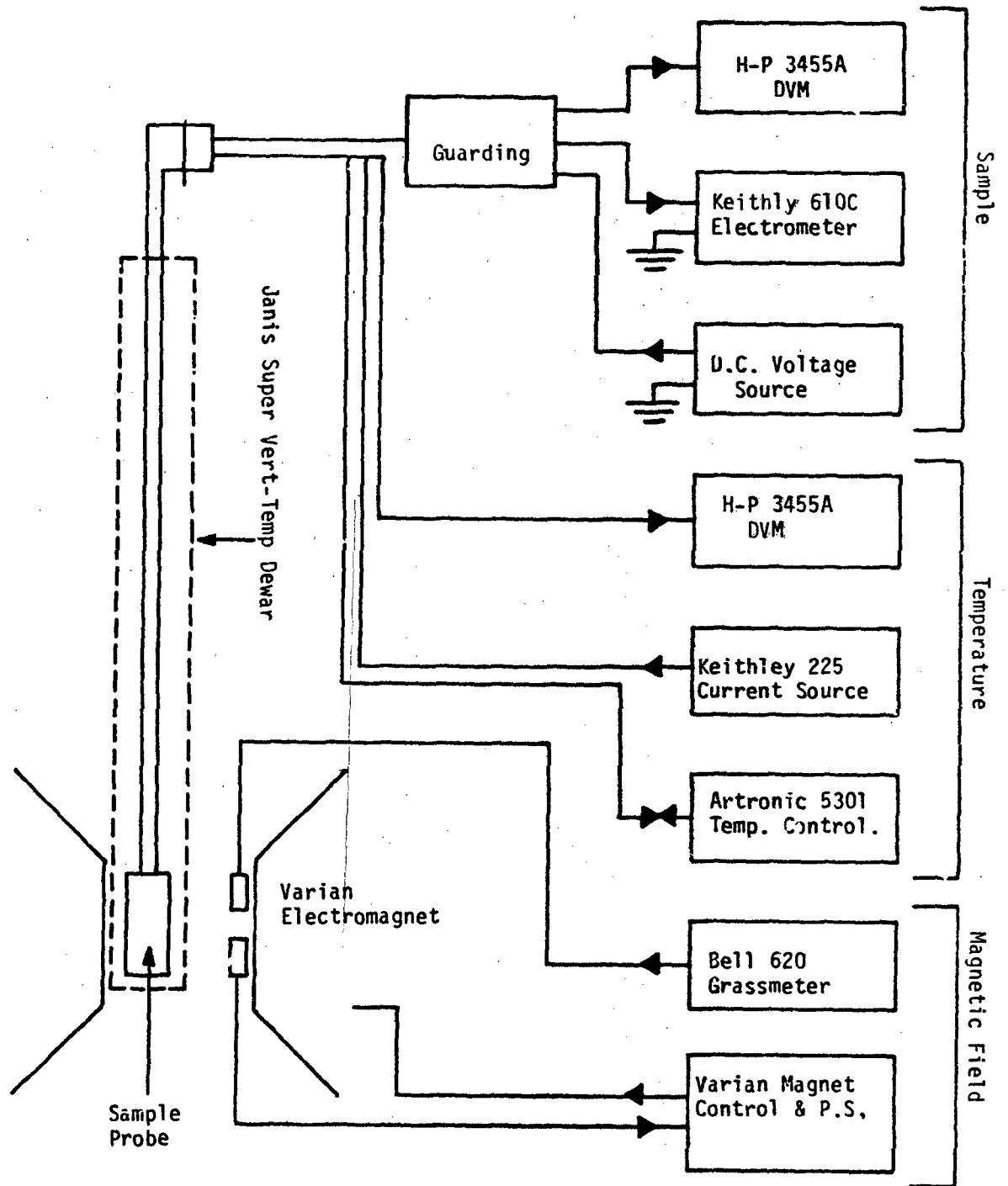


Figure 7. Resistivity and Hall Coefficient Measurement System

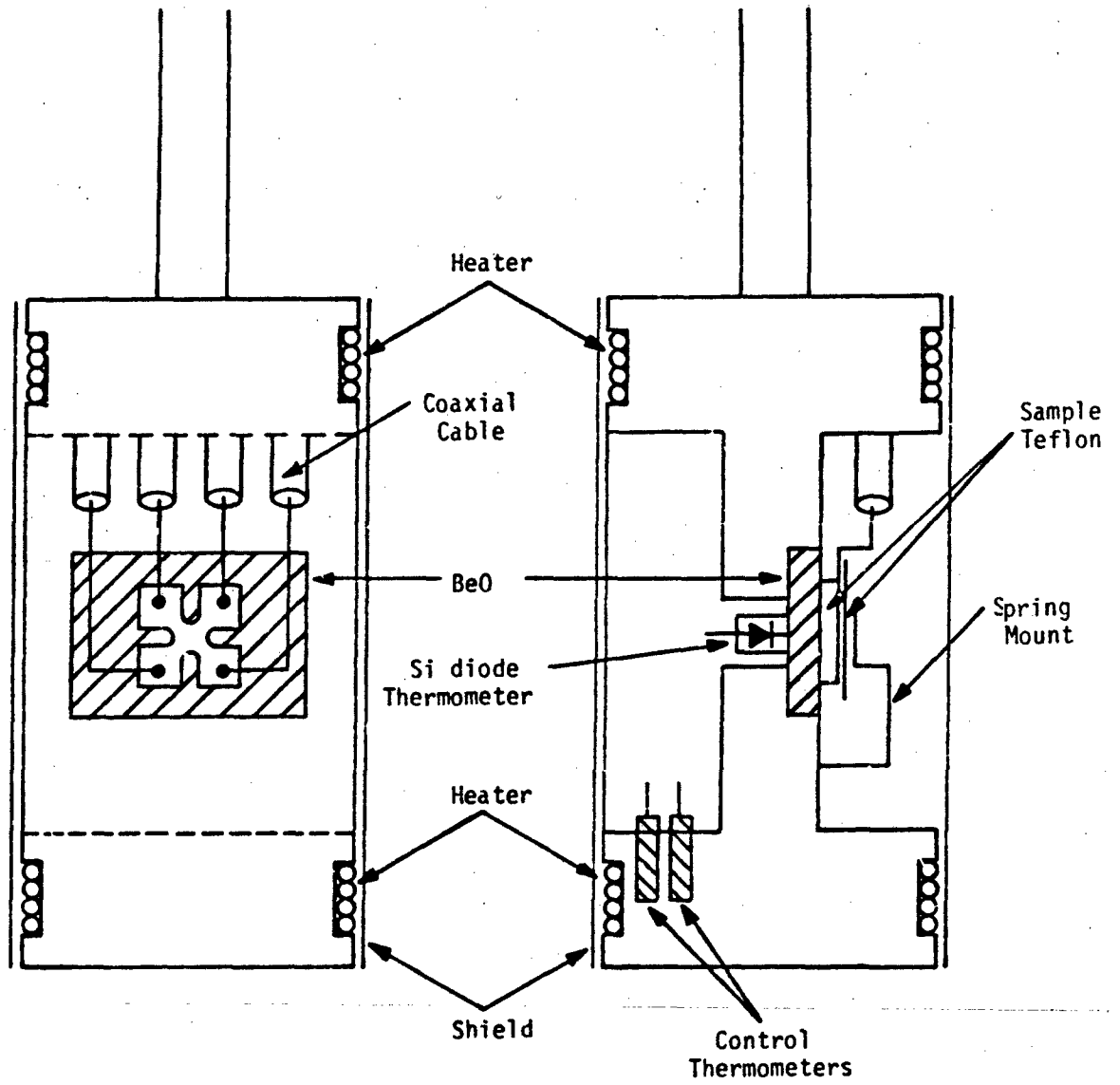


Figure 8. Sample Holder

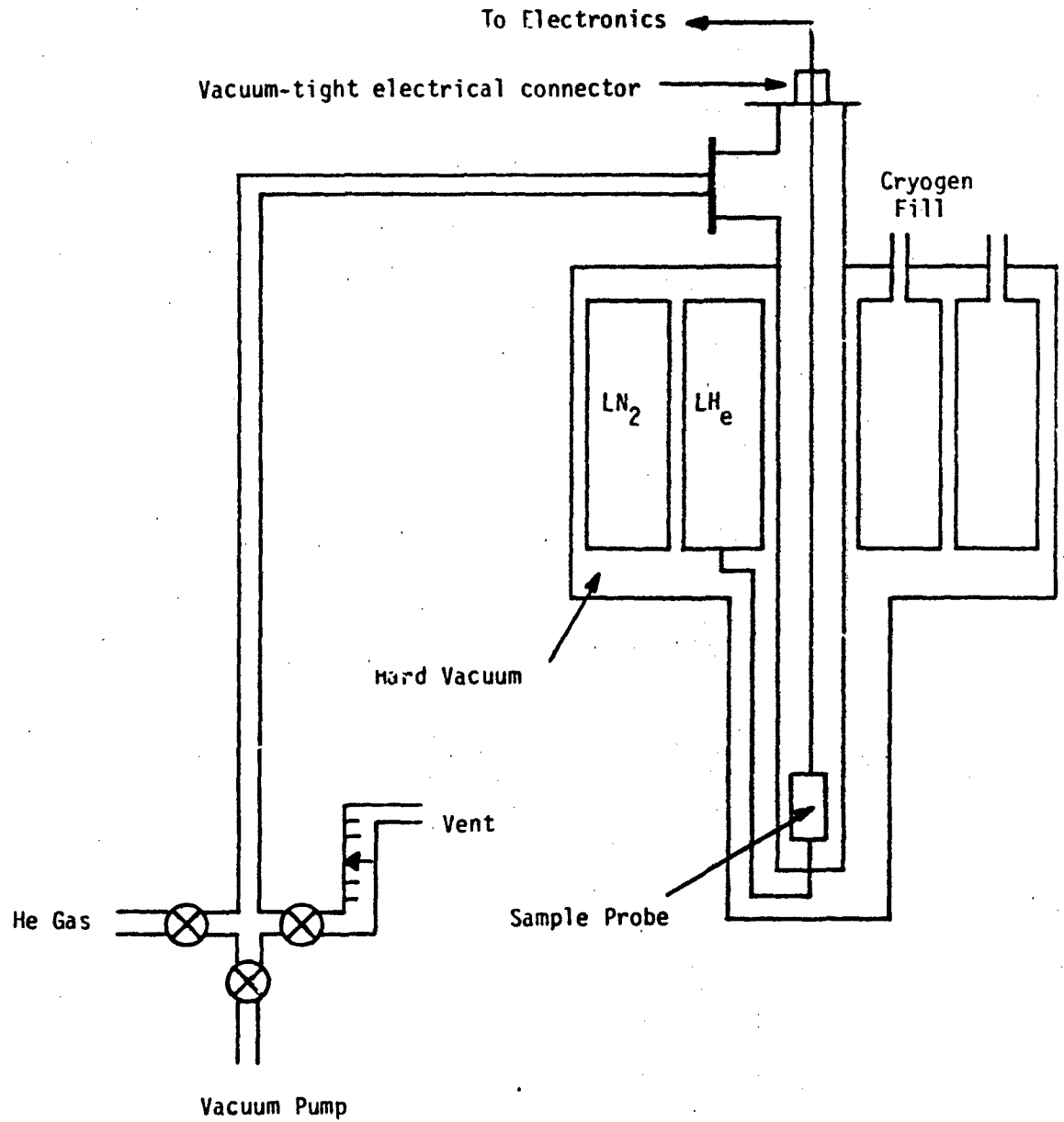


Figure 9. Dewar Support System

## SECTION V

## RESULTS

Isothermal anneals were performed on samples of the Hughes material, H1, at three temperatures, 450, 525 and 600 C. Annealing time varied from a minimum of 15 minutes to a maximum of 20 hours. In addition, 1-hour anneals were performed at 550, 650 and 750 C on other samples from H1 for an isochronal anneal set. The results of these experiments will be presented in this report in detail. Isochronal anneals from 450 to 850 C were also performed on samples from boules V1, V2 and W1 and will form the basis of a future report. The results of this latter study will be reported here only for comparison. In addition to the Hall effect measurements, photoluminescence, infrared absorption and photoconductivity experiments were performed on samples from V1 and W1 by members of the Laser & Optical Materials Branch and by the University of Dayton Research Institute. These will be reported in detail in a future report and quoted here only when necessary.

The results of the 450 C isothermal anneals on H1 are presented in Table 5 and Figure 10. No shallow acceptor levels were detected after any of the anneals, and the donor concentration appears stable. Similar results occurred in the early stages of the 525 C anneal study as well with only gallium being detected from 1/4 to 1 hour with the donors remaining reasonably stable. After the 2-hour anneal, however, the Ga-X level with an average activation energy of about 0.054 ev. was detected as well, and the donors started to anneal out. The Ga-X level remained reasonably constant out to 20 hours and the donors stabilized after 5 hours. These results are presented in Table 6 and Figure 11. We note here that the energies from Hall effect analysis for both the Ga and Ga-X levels were lower than the generally accepted values.  $E_{Ga}$  varied between 0.069 and 0.072 ev. with an average around 0.071 and  $E_{GaX}$  varied between .053 and 0.56 ev. The accepted values are  $E_{Ga} = 0.073$  and  $E_{GaX} = 0.057$ . Our energies improved as the donor concentration decreased with longer and higher temperature anneals. We attribute this error to the effect of high compensations.

TABLE 5

450°C ANNEAL FITTING RESULTS

| Total Time (hrs) | $N_D$ ( $\text{cm}^{-3}$ ) | $N_{Ga}$ ( $\text{cm}^{-3}$ ) |
|------------------|----------------------------|-------------------------------|
| 1.0              | $2.1 \times 10^{16}$       | $3.6 \times 10^{16}$          |
| 2.0              | $1.8 \times 10^{16}$       | $2.8 \times 10^{16}$          |
| 5.0              | $1.9 \times 10^{16}$       | $3.1 \times 10^{16}$          |

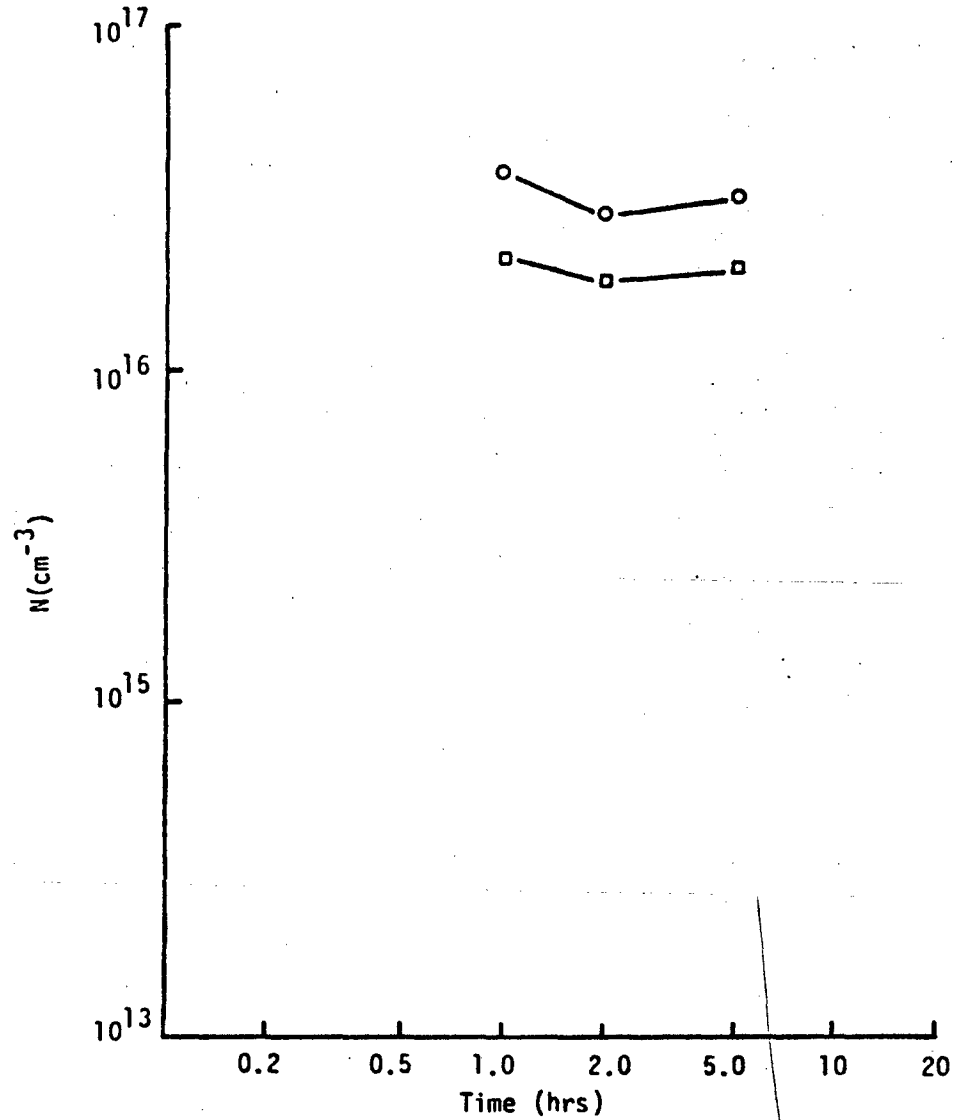


Figure 10. Concentration of Centers vs. Anneal Time, 450 C  
 ○ -  $N_{Ga}$ , □ -  $N_{Donors}$

TABLE 6

525°C ANNEAL FITTING RESULTS

| Total Time (hrs) | $N_D$ ( $\text{cm}^{-3}$ ) | $N_{Ga}$ ( $\text{cm}^{-3}$ ) | $N_{GaX}$ ( $\text{cm}^{-3}$ ) |       |
|------------------|----------------------------|-------------------------------|--------------------------------|-------|
| 0.25             | $8.4 \times 10^{15}$       | $2.2 \times 10^{16}$          | ---                            | -.602 |
| 0.5              | $6.6 \times 10^{15}$       | $2.1 \times 10^{16}$          | ---                            | -.301 |
| 1.0              | $4.7 \times 10^{15}$       | $2.1 \times 10^{16}$          | ---                            | .0    |
| 2.0              | $1.6 \times 10^{15}$       | $2.0 \times 10^{16}$          | $1.6 \times 10^{15}$           | 0.301 |
| 5.0              | $7.5 \times 10^{14}$       | $2.0 \times 10^{16}$          | $2.3 \times 10^{15}$           | 0.699 |
| 10.0             | $6.1 \times 10^{14}$       | $2.3 \times 10^{16}$          | $1.3 \times 10^{15}$           | 1.00  |
| 20.0             | $9.1 \times 10^{14}$       | $2.4 \times 10^{16}$          | $1.1 \times 10^{15}$           | 1.301 |

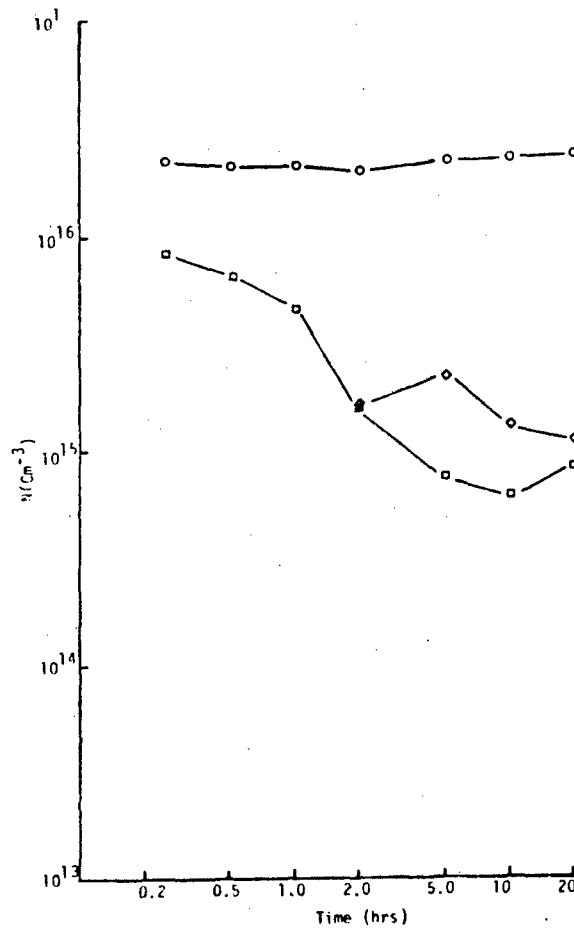


Figure 11. Concentration of Centers vs. Anneal Time, 525 C

○ -  $N_{Ga}$ , ◇ -  $N_{GaX}$ , □ -  $N_{Donors}$

Our empirical scattering factor,  $r$ , was developed for very low compensation with concomitantly lower ionized impurity scattering and so it is conceivable that the additional ionized impurity scattering at lower temperatures in these samples would require a further modified scattering factor. We do not believe that the concentrations are seriously affected because  $N_{Ga}$  does not vary appreciably as the donor concentration decreases.

The level at 0.054 ev. was conclusively identified as Ga-X despite the error in energy by comparing the results of Hall effect analysis on samples from V1 and W1 with infrared absorption results. The absorption experiment revealed excited state lines of Ga-X at the proper energies in samples from the same boules with identical irradiations and anneals to the Hall effect samples.

The results of the 600 C anneal study are presented in Table 7 and Figure 12. For the first time the  $A_1$  and  $A_2$  levels of Young et al. (References 6, 7, 8) are seen. The shortest anneals are somewhat ambiguous in that only  $A_2$  (0.04 ev.) was detected after 1/4 hour and only  $A_1$  (0.027 ev.) after 1/2 hour while both were detected for the 1, 2 and 5 hour anneals. The 1/2 hour data was very noisy for some reason and a truly satisfactory fit was never obtained so this could explain the absence of  $A_2$  at this time. No evidence of the Ga-X level was detected at any time for 600 C although absorption experiments did reveal Ga-X after 600 C anneal for 1 hour on V1 samples. Absorption experiments are presently planned for a sample from H1 annealed at 600 C for 1 hour. The donors in the 600 C set of runs show an anomalous rise at the last two points, 10 and 20 hours. This is unexplained at present but a similar effect was seen in isothermal anneals at 600 C on Hall samples from W1. There is also a rise in  $N_d$  at the last data point in the 525 C set. The donor concentrations for all the isothermal runs in this study are shown in Figure 13. Note that there is a consistent drop in donor concentration with both temperature and time, except for the rises mentioned above. The rate of decrease with time appears to increase with increasing temperature. This would be expected if we are looking at the annealing of one type of center.

TABLE 7

600 C ANNEAL FITTING RESULTS

| Total Time (hrs) | $N_D$ ( $\text{cm}^{-3}$ ) | $N_{Ga}$ ( $\text{cm}^{-3}$ ) | $N_{A2}$ ( $\text{cm}^{-2}$ ) | $N_{A1}$ ( $\text{cm}^{-3}$ ) |
|------------------|----------------------------|-------------------------------|-------------------------------|-------------------------------|
| 0.25             | $1.5 \times 10^{15}$       | $2.0 \times 10^{16}$          | $1.6 \times 10^{15}$          | ---                           |
| 0.5              | $2.2 \times 10^{15}$       | $1.9 \times 10^{16}$          | ---                           | $2.2 \times 10^{15}$          |
| 1.0              | $2.3 \times 10^{14}$       | $2.0 \times 10^{16}$          | $1.5 \times 10^{14}$          | $3.2 \times 10^{14}$          |
| 2.0              | $1.2 \times 10^{14}$       | $2.1 \times 10^{16}$          | $1.7 \times 10^{14}$          | $1.3 \times 10^{14}$          |
| 5.0              | $6.3 \times 10^{13}$       | $2.3 \times 10^{16}$          | $1.2 \times 10^{14}$          | $9.3 \times 10^{13}$          |
| 10.0             | $1.4 \times 10^{14}$       | $2.1 \times 10^{16}$          | $1.4 \times 10^{14}$          | ---                           |
| 20.0             | $1.6 \times 10^{14}$       | $2.1 \times 10^{16}$          | $1.6 \times 10^{14}$          | ---                           |

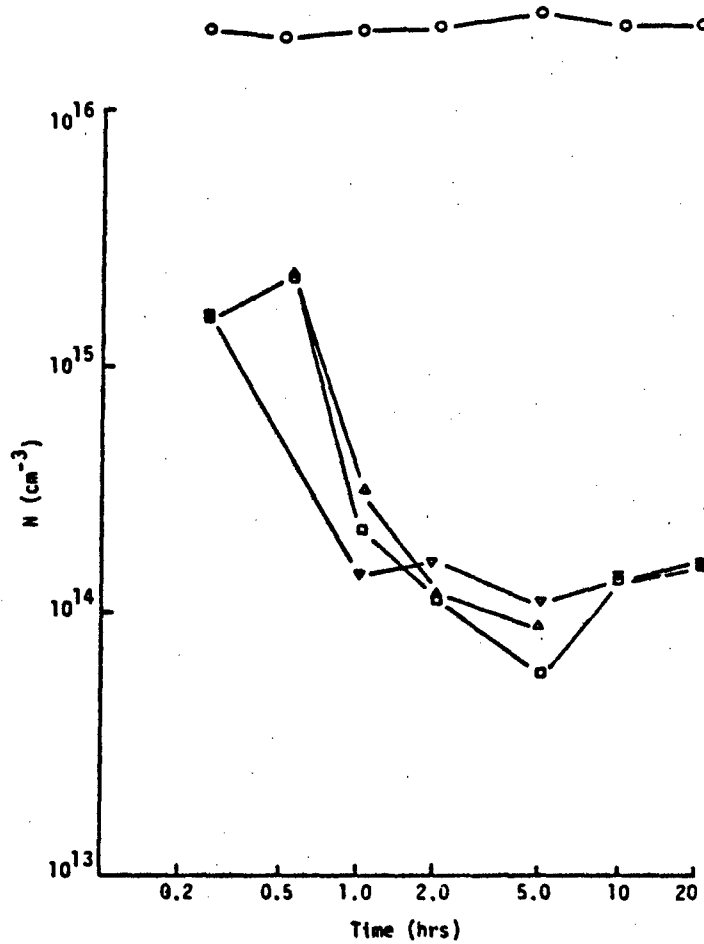


Figure 12. Concentration of Centers vs. Anneal Time, 600 C  
 O -  $N_{Ga}$ ,  $\nabla$  -  $N_{A2}$ ,  $\Delta$  -  $N_{A1}$ ,  $\square$  -  $N_{Donors}$

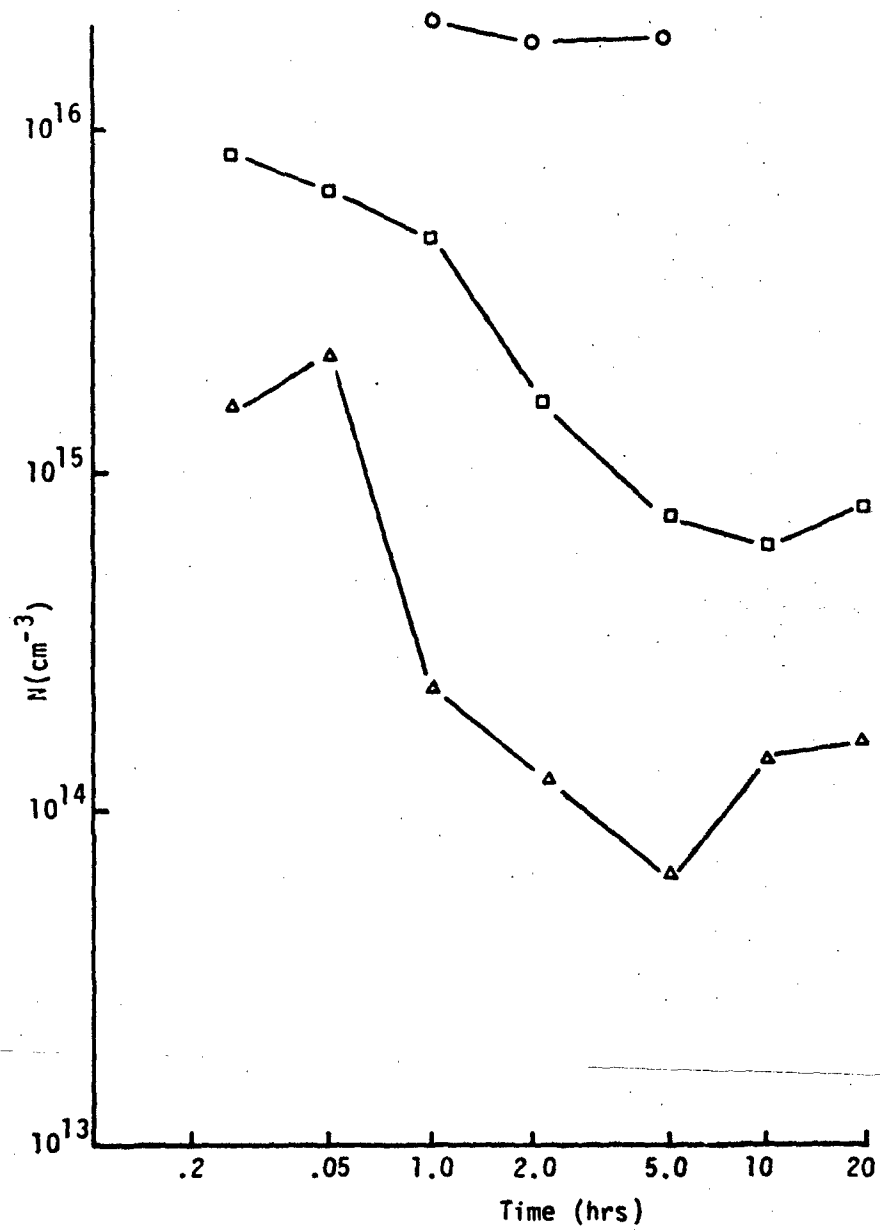


Figure 13. Effect of Temperature and Time on the Annealing of Donors in NTD, p-type Si. o - 450 C, □ - 525 C, Δ - 600 C

The 1 hour results from each isothermal set have been combined with additional results from other samples from H1 annealed for 1 hour at 550, 650, 750 and 840 C to produce an isochronal set. These results are shown in Figure 14 and tabulated in Table 8. This set is not as informative as would have been expected because of the rapid appearance and disappearance of  $A_1$  and  $A_2$ , but coupling this with the isothermal results, it does appear that  $A_2$  is more stable than  $A_1$  although this is not conclusive. Ga-X was not detected in any of the 1 hour runs, probably because of the high donor concentrations at the lower temperatures.

Note that there is also an anomalous behavior in the results for the energy of the  $A_2$  level which is particularly obvious in the 600 C isothermal results. The shorter anneals gave the energy as  $0.040 \pm .002$ , but after 2 hours, the energy was consistently  $0.035 \pm .002$  ev. This energy also appeared in some of the analyses for the V1 and W1 samples as well. At present we cannot tell whether this is real and we are seeing an additional acceptor or if it is only due to r-factor corrections in the analysis.

TABLE 8

ISOCHRONAL ANNEAL RESULTS, ONE-HOUR ANNEALS

| T(°C) | $N_D$ (cm <sup>-3</sup> ) | $N_{Ga}$ (cm <sup>-3</sup> ) | $N_{A2}$ (cm <sup>-3</sup> ) | $N_{A1}$ (cm <sup>-3</sup> ) |
|-------|---------------------------|------------------------------|------------------------------|------------------------------|
| 450   | $2.1 \times 10^{16}$      | $3.6 \times 10^{16}$         | ---                          | ---                          |
| 525   | $4.7 \times 10^{15}$      | $2.1 \times 10^{16}$         | ---                          | ---                          |
| 550   | $4.0 \times 10^{15}$      | $2.5 \times 10^{16}$         | ---                          | ---                          |
| 600   | $2.3 \times 10^{14}$      | $2.0 \times 10^{16}$         | $1.5 \times 10^{14}$         | $3.2 \times 10^{14}$         |
| 650   | $7.8 \times 10^{13}$      | $2.6 \times 10^{16}$         | $1.8 \times 10^{14}$         | $1.4 \times 10^{14}$         |
| 750   | $1.5 \times 10^{14}$      | $2.9 \times 10^{16}$         | ---                          | ---                          |
| 840   | $9.5 \times 10^{13}$      | $2.1 \times 10^{16}$         | ---                          | ---                          |

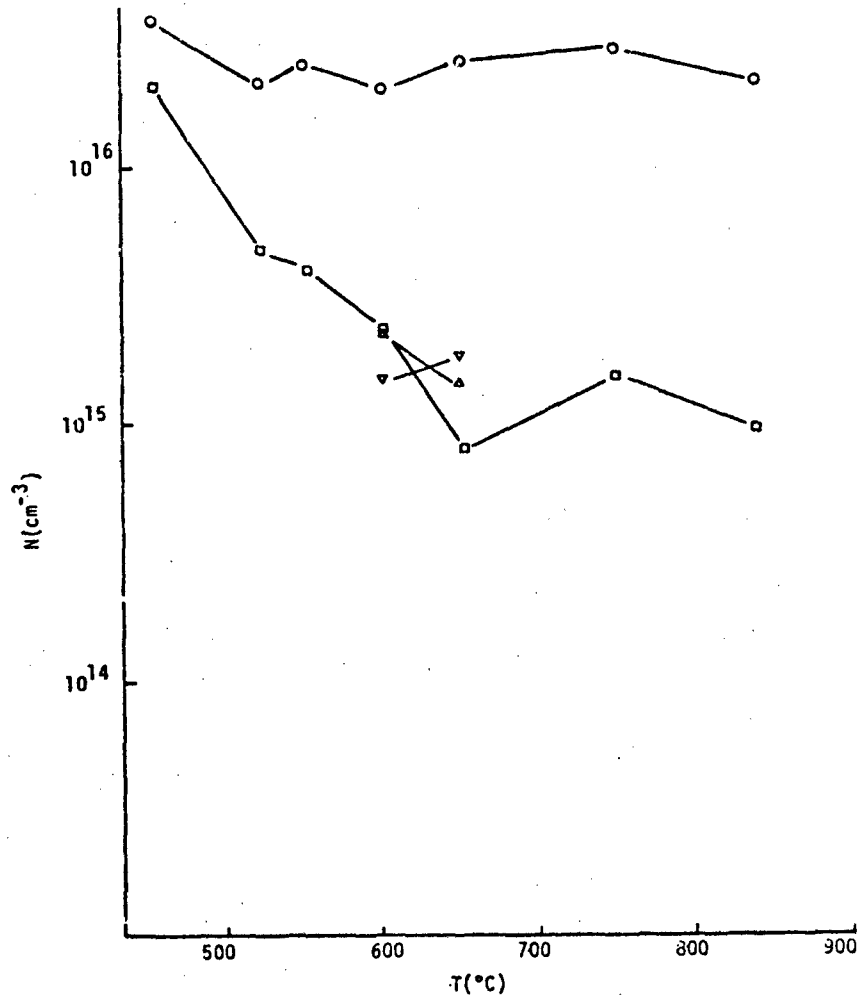


Figure 14. One-hour anneal results for NTD, p-type Silicon

○ -  $N_{Ga}$ , □ -  $N_D$ , ▽ -  $N_{A2}$ , △ -  $N_{A1}$

## SECTION VI

## DISCUSSION

The 450 C and 525 C anneal results are not difficult to explain, although these results were somewhat unexpected. The extremely high donor concentrations at all 450 C anneals indicate large amounts of lattice damage in the form of stable complexes, for simple defects such as isolated vacancies, interstitials and divacancies would have annealed out by this temperature. The concentration of donors in this sample is an order of magnitude higher than that detected in similar material irradiated at the University of Missouri. This was unexpected because the thermal to fast neutron ratios of the two light water reactors are similar, 22 for TA&M and 20-30 for MURR. The principal difference between the two reactors appears to be the flux-MURR is a relatively high flux reactor compared to the TA&M reactor. This can explain the difference if one considers the effect of flux on the temperature of the samples during irradiation. It is a well-known fact that samples heat up during neutron irradiation in a reactor if not cooled by direct contact with the bath water or by other means. This is primarily due to gamma ray absorption, which is higher in the high flux reactors (Reference 24).

If the temperatures of the samples were different during irradiation, different defects could be formed. Gamma ray irradiation could also produce different defects. These defects, which are not identified by Hall effect analysis, would probably show different annealing behavior. At present, we believe that the relatively lower irradiation temperature at the TA&M reactor results in a significantly higher number of primary defects which, in turn, form larger clusters than during the higher temperature irradiation at MURR. Optical experiments are underway in our laboratory to verify these expectations. If our postulate is correct, the donors seen at 450 C in the TA&M samples would be due to large, stable clusters which are not formed at MURR. When the larger clusters eventually anneal out, one would expect them to form dislocation loops and such that would be detectable by electron microscopy even after anneals above 850 C.

Because of the high concentration of donors in the samples used in this study, we could not detect any shallow acceptors present in concentrations below about  $1 \times 10^{16} \text{ cm}^{-3}$  in the 450 C data by Hall analysis. Measurements on MURR samples annealed at 450 C reveal Ga-X at a concentration around  $1 \times 10^{15} \text{ cm}^{-3}$ , so one can reasonably assume that this acceptor is present at 450 C in our samples as well but is completely compensated by the donors. Further evidence for the validity of this assumption is found in the 525 C data, where we do detect the Ga-X level, but only after a 2-hour anneal. The acceptor appears reasonably stable with time at this temperature while the donors are decreasing monotonically, indicating that Ga-X was present all along but could not be seen by Hall effect analysis due to overcompensation.

The presence of Ga-X in neutron irradiated material can be explained in terms of the substitutional gallium-substitutional carbon complex model in the following manner. Initially, Ga and C atoms are widely separated; therefore, no Ga-X would be detected in as-grown material. This is verified by measurements in our laboratory on over twenty different boules of float zone Si:Ga from four different sources. None of these measurements showed significant amounts of Ga-X. Once the material is irradiated, large numbers of silicon vacancies are formed. Work by Watkins (References 11, 25) indicates that  $\text{Si}_i$ 's are unstable at room temperature. These defects migrate interstitially until they combine with an impurity. This complex is also unstable and decays by an exchange of the substitutional impurity and the interstitial silicon, leaving only an interstitial impurity. Ga interstitials start to anneal at around 230 C (Reference 25). Carbon interstitials start to return to substitutional sites at around 250 C (Reference 26). Before these interstitials return to substitutional sites, they are reasonably mobile and it is postulated that there is an attraction between group III atoms and carbon atoms, possibly due to charged states of the interstitial states, to some deformation attraction, or to migration to vacancy clusters such as the divacancy. Regardless of the mechanism, interstitial gallium and carbon end up near each other and remain there when they return to substitutional sites, thus forming Ga-X.

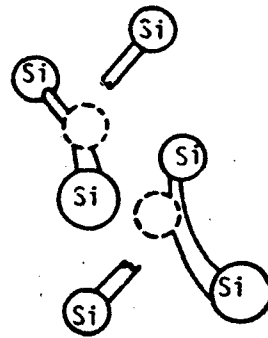
The shallow levels labeled  $A_1$  and  $A_2$  were detected in the 600 C data and the 650 C, 1-hour run, but were both gone by 750 C. In fact, all shallow acceptors were annealed out by 750 C. Both  $A_1$  and  $A_2$  were detected at 600 and 650 C. They might be present at lower temperatures and not detectable due to compensation by donors. Experiments on samples from boules VI and W1 irradiated at MURR and therefore with lower donor concentrations, indicate that these acceptors develop somewhere between 450 C and 550 C. This agrees with the results of the HRL group as well. That group thought that  $A_1$  and  $A_2$  were due to some complex of gallium and multiple vacancies. We agree with this.

These levels must be complexes of some sort because there are no elements that show such low electrical activation energy. Simple defects such as vacancies and interstitials anneal out well before  $A_1$  and  $A_2$  become visible. We can also eliminate many other complexes from consideration for various reasons. A gallium-gallium complex is unlikely because there would be some indication of this in heavily doped material and no such levels have been reported. Other gallium-acceptor or gallium-donor complexes can be eliminated because there are no other electrically active impurities present in a high enough concentration to produce either level. Only carbon and oxygen are present at levels high enough to yield the concentrations seen. It is unlikely that carbon is involved because it has already returned to substitutional sites as evidenced by the presence of Ga-X at 525 C and substitutional gallium-substitutional carbon nearest neighbors complex is the Ga-X level itself. Higher order substitutional complexes seem unlikely due to the high concentrations of  $A_1$  and  $A_2$  as well as the concentration of carbon in the starting material, given by HRL as around  $2 \times 10^{15} \text{ cm}^{-3}$ . Oxygen is known to form various complex with a variety of other defects (References 27, 28, 29) and is present in the high  $10^{15} \text{ cm}^{-3}$  range as reported by HRL. Carbon forms complexes with oxygen such as  $C_s-O_i$  and  $C_s-2O_i$  as reported by Bean and Newman from IR absorption measurements (Reference 27). These complexes are seen at elevated temperatures and so could be responsible for  $A_1$  and  $A_2$  but one would then expect to see these in electron irradiated material as well and so such acceptors have been reported in the literature for that type of irradiation.

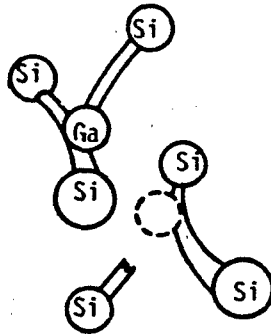
Gallium is apparently involved in the complexes because the HRL group reported a convincing correlation between the concentrations of  $A_1$  and  $A_2$  and that of gallium. Because we see gallium activation at 450 C, the gallium in the complexes is probably substitutional as well. So a  $Ga_S-O$  complex is a possibility, but we have trouble seeing why this should not be present in as-grown Czochralski material where the oxygen concentration is several orders of magnitude higher than that in the float zone material used in this study.

What we are left with is a substitutional gallium atom (or two) complexed with an intrinsic defect of some sort. Interstitials are annealed out well before gallium goes substitutional and so they can be eliminated from consideration. Vacancies and vacancy complexes are intriguing. An Al-V complex has been reported in electron irradiated material by EPR (Reference 25), but was seen to anneal out between 300 to 400 C. One may argue that a Ga-V complex will anneal at a similar temperature and, therefore, cannot be responsible for  $A_1$  or  $A_2$ ; but the divacancy,  $V_2$ , is more stable than the single vacancy. Again, though, the  $V_2$  anneals before  $Ga_i$  return to substitutional sites, but there is a possible source for  $V_2$  at elevated temperatures in neutron irradiated material.

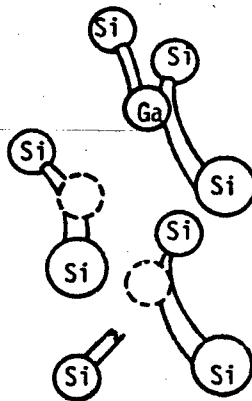
Neutron irradiation produces large vacancy clusters which do not disappear until temperatures above 450 C. This is obvious from our annealing studies presented in the previous section. The donors seen must be due to some sort of complex or other and they do start to break up about 450 C. The complex annealing kinetics of the donors is indicative of an assortment of clusters. We propose that these clusters anneal, at least partially, by "evaporating" its relatively stable  $V_2$  which then migrates through the lattice. This has been suggested by Watkins (Reference 30). We further postulate that the  $V_2$ 's can be captured by  $Ga_S$ 's and produce one of the shallow acceptors. Figure 15 shows the divacancy and the Ga- $V_2$  complex as well as Ga-V. Whether, such a complex could yield an acceptor is an open question and must be



DIVACANCY



Ga-VACANCY



Ga-DIVACANCY

Figure 15. Structure of  $V_2$ , Ga-V and Ga- $V_2$

resolved before this model can be taken seriously, but if it does, it should yield precise energy levels. The lowering of the Ga activation energy might be due to a process similar to the proposal for the X levels by Searle et al. (Reference 12).

We can only speculate at this time on which acceptor could be related to the Ga- $V_2$  complex, but the activation energy of  $A_1$  is found to be very consistent between samples and anneals while that of  $A_2$  fluctuates. If we identify Ga- $V_2$  with  $A_1$ , then  $A_2$  could be due to gallium atoms complexing with higher order vacancy clusters. There would be several non-equivalent nearest-neighbor sites for a defect like a penta-vacancy and this might explain the variations in  $E_{A_2}$ . We do not feel that  $A_1$  and  $A_2$  are due to different charge states of the same level because of the different annealing kinetics of the two levels.

## SECTION VII

## CONCLUSIONS

The annealing behavior of neutron transmutation doped silicon has been studied, primarily by isothermal anneals at 450 C, 525 C and 600 C. Several shallow acceptor levels have been studied. The Ga-X level at 0.057 ev. was seen after two hours at 525 C. This confirms the earlier discovery of Ga-X in NTD Si:Ga by Rome et al. (Reference 14) in material irradiated at a different reactor, as well as the prediction of Newman (Reference 30) that neutron irradiation should produce this level.

Two shallower acceptors at 0.026 and 0.040 ev. were seen in anneals at 600 C in agreement with previous work of researchers at HRL. These have been attributed to a Ga-V<sub>2</sub> complexes and higher order vacancy complexes. The annealing behavior of these levels is complex.

The discovery that the NTD process produces Ga-X is important technologically because this shallow acceptor is long-lived and might well remain after high-temperature anneals, adversely affecting the lifetime of IR detectors fabricated from NTD material. The best way to avoid this is to use low-carbon material and prevent carbon contamination during growth. The shallower levels, A<sub>1</sub> and A<sub>2</sub>, appear to be completely removed by anneals at 750 C and should not influence the detector properties.

Effects of various reactors are also evident. This is particularly obvious in the production and annealing of donors. The reactor with the higher flux and, therefore, the higher irradiation temperature results in few donors at 450 C, and all temperatures higher than this until complete recovery at 850 C. Both reactors produced the same shallow acceptors but the concentrations were higher for the higher flux reactor, exactly the opposite effect as that for the donors. This has not been explained yet.

AFWAL-TR-83-41 B

Further experimental studies are needed to verify the Ga-V<sub>2</sub> model. Isothermal studies at two temperatures where the A<sub>1</sub> and A<sub>2</sub> levels are detectable should give valuable information on the annealing kinetics. Theoretical studies should also be instituted to verify that Ga-V<sub>2</sub> is, in fact, an acceptor.

## REFERENCES

1. W. G. Pfann, Zone Melting (Wiley, New York, 1966).
2. M. Tanebaum and A. D. Mills, Jour. of Electrochem. Soc. 108, 171(1961).
3. J. M. Meese, ed., Neutron Transmutation Doping in Semiconductors (Plenum Press, New York, 1979).
4. Jens Guldbery, ed., Neutron-Transmutation-Doped Silicon (Plenum Press, New York, 1981).
5. R. N. Thomas, T. T. Braggins, H. M. Hobgood, and W. J. Takai, J Appl. Phys. 49, 2811 (1978).
6. M. H. Young, R. Baron and O. J. Marsh, in Neutron Transmutation Doping in Semiconductors, J. M. Meese, ed. (Plenum Press, New York, 1979), p. 335.
7. M. H. Young, O. M. Stafsudd, K. L. Brower, O. J. Marsh and R. Baron, in Neutron-Transmutation-Doped Silicon, Jens Guldbery, ed., (Plenum Press, New York, 1981).
8. M. H. Young, O. J. Marsh and R. Baron, J. Appl. Phys. 50 3755 (1979).
9. R. A. Smith, Semiconductors, 2nd ed. (Cambridge University Press, Cambridge, 1979).
10. J. C. Corelli, in Neutron Transmutation Doping in Semiconductors, J. M. Meese, ed. (Plenum Press, New York, 1979), p. 36.
11. G. D. Watkins, in Lattice Defects in Semiconductors, P. Baruch, ed. (Dunod, London, 1965), p. 97.
12. C. W. Searle, M. C. Ohmer and P. M. Hemenger, Sol. St. Comm. 44, 1597 (1982).
13. V. Swaminathan, J. E. Lang, P. M. Hemenger and S. R. Smith, Appl. Phys. Lett. 35, 184 (1979).
14. John J. Rome, W. C. Mitchel, Gail J. Brown, David W. Fischer, M. C. Ohmer and T. L. Peterson, J. Appl. Phys. 41, 254 (1982).
15. E. H. Hall, Am. J. Math. 2, 287 (1879).
16. C. Kittel, Introduction to Solid State Physics, 4th ed. (Wiley, New York, 1971), p. 287.
17. L. J. van der Pauw, Phillips Tech. Rpts. 13, 1 (1958).

## REFERENCES (Concluded)

18. K. Seeger, Semiconductor Physics (Springer-Verlag, New York, 1973).
19. F. L. Madarasz, J. E. Lang and P. M. Hemenger, J. Appl. Phys. **52** 4646 (1981).
20. Phillip R. Bevington, Data Reduction and Error Analysis for the Physical Sciences (McGraw-Hill, New York, 1969).
21. Emulsitone Co., Whippany, New Jersey.
22. Patrick M. Hemenger, Rev. Sci. Instrum. **44**, 698 (1973).
23. D. Colman, Rev. Sci. Instrum. **34**, 1946 (1968).
24. J. Baker, private communication.
25. G. D. Watkins, Phys. Rev. **155**, 802 (1967).
26. K. L. Brower, Phys. Rev. B **9**, 2607 (1974).
27. A. R. Bean and R. C. Newman, J. Phys. Chem. Solids **33**, 255 (1972).
28. R. E. Whan, J. Appl. Phys. **37**, 3378 (1966).
29. C. S. Fuller and F. H. Doleiden, Phys. Rev. **29**, 1264 (1958).
30. R. C. Newman, in Neutron-Transmutation-Doped Silicon, Jens Buldberg, ed. (Plenum, New York, 1981), p. 83.